Summary We consider the Dirichlet problem for the Laplace equation in a 2D (3D) starlike domain. Such a domain can be interpreted as a non-isotropically stretched unit circle (sphere). We write down the explicit solution in terms of a Fourier series whose coefficients are determined by solving an infinite system of linear equations depending on the boundary data. Similar results are obtained for the solution of the Dirichlet problem for the Helmholtz equation. Numerical experiments show that our method guarantees almost everywhere convergence, whenever the boundary data are sufficiently smooth, in accordance with the results proved by L. Carleson.

2010 Mathematics Subject Classification: 35J05, 35J25.
Key Words and phrases: Dirichlet problem, Laplace equation, starlike domain.

Diego Caratelli
International Research Centre for Telecommunications and Radar
Delft University of Technology
Mekelweg 4 – 2628 CD Delft, the Netherlands
e-mail: d.caratelli@tudelft.nl

Bruna Germano
Dipartimento di Metodi e Modelli Matematici
"Sapienza" Università di Roma
Via A. Scarpa, 14 – 00161 Roma, Italia
e-mail: germano@dmmm.uniroma1.it

Johan Gielis
Institute for Wetland and Water Research Faculty of Science
Radboud University Nijmegen
Heyendaalseweg 135 – 6525 AJ Nijmegen, The Netherlands
email: Johan.gielis@mac.com

Matthew X. He
Nova Southeastern University
3301 College Avenue
Fort Lauderdale, FL 33314-7796, U.S.A.
e-mail: hem@nova.edu

Pierpaolo Natalini
Dipartimento di Matematica
Università degli Studi di Roma Tre
Largo San Leonardo Murialdo 1 – 00146 Roma, Italia
e-mail: natalini@mat.uniroma3.it

Paolo E. Ricci
UniNettuno University
Corso Vittorio Emanuele II, 39
00186 Roma, Italia
e-mail: paoloemilioricci@gmail.com

In memoriam *Francesco Ricci* *and* *Elvira (Nina) Garrone.*

Contents

Introduction

These Lecture Notes address numerical solutions of long standing problems in mathematical physics. The search for a uniform method for solving classical boundary value problems (BVP) has occupied many eminent researchers, but exact solutions are limited to specific shapes only (domains satisfying special symmetry properties such as circle, spheres, intervals, etc.). In these Lecture Notes we show that the use of a suitable change of coordinates (here referred to as anisotropically stretched polar or spherical coordinates) provides a uniform method to apply the classical Fourier theory even in the case of general normal polar (e.g., starlike) domains. In this way we are able to achieve the "exact" solution of many classical BVP in terms of Fourier series, where "exact" means that we can approximate a prescribed finite number of coefficients of the Fourier expansion of the solution as closely as we wish.

Hence, the classical Dirichlet, Neumann, Robin problems for the Laplace or Helmholtz equation are always the same, independent of the shape of the domain in which they are considered, provided that this domain can be reduced to a circle (or a sphere) by a suitable change of coordinates. This idea traces back to Euler, Gauss and the Italian mathematician A.M. Ferrari, but was considered as a more general framework in the early 19th century by Gabriel Lamé (1795-1870) who foresaw "l'avènement futur d'une science rationnelle unique", i.e. a rise to the throne of a unique rational science, which at present can be identified with Mathematical Physics.

Lamé, like Fourier, was professor at the École Polytechnique and many of his achievements are connected with the distribution of heat. His influence on science continues to be impressive. In particular, Lamé's work on curvilinear coordinates (considered by Darboux as immortal) generalized the early work of Euler on curves and of Gauss on surfaces opening the door for Cartan's moving frames [1]. Cartan himself considered Lamé as a cofounder of the Riemannian geometry. Lamé envisaged that, from the mathematical point of view, the study of a physical system reduces to the study of a system of curvilinear coordinates, adapted to the given physical situation (providing the initial geometrical support for a physical system). The study of that physical problem, adapted with the appropriate system of curvilinear coordinates then becomes the characterization of the system of differential invariants or the calculation of the Laplacian in curvilinear coordinates. In his view this reduces to one equation only, namely the Poisson equation in curvilinear coordinates, with boundary conditions.

Earlier, at the age of 21 Lamé had introduced equations of the type $x^n + y^n = 1$ and noted that a special choice of exponents gave a uniform description of all conic sections [2]. These Lamé curves gave the possibility of defining measures and metrics based on powers other than two. In these Lecture Notes we give examples of "stretched" polar or spherical coordinates using so called supershapes (or more generally Gielis curves or surfaces [3]), which actually generalize Lamé curves and surfaces. Lamé-Gielis curves and surfaces describe natural shapes in a uniform way, as a generalization of conic sections, and they give natural metrics in Riemann-Finsler geometry and all natural processes that are modeled in this way. They provide intrinsic coordinate systems or a geometric support adapted to the shape and so, almost two centuries after Lamé and Fourier, in a straightforward way, their thoughts and visions are united here in a straightforward (and unexpected) way. In this historical perspective the solution could be considered canonical.

This computational method and the relevant numerical accuracy are documented in these Lecture Notes by application to different examples. Here we focus on Laplace and Helmholtz equations but the same method can be extended to other types of BVP and other types of descriptors. Especially Lamé-Gielis curves and surfaces will benefit from this computational method, combining a uniform description with a straightforward computational method, for a wide range of applications.

Acknowledgments. We would like to express our sincere gratitude to Prof. Dr. George Jaiani of the Tbilisi State University who first helped and encouraged one of us (P.E. R.) to explore the present numerical technique.

References

[1] R. Guitart, Les coordonnées curvilignes de Gabriel Lamé, réprésentations des situation physiques et nouveaux objects mathématiques. In: Gabriel Lamé: Les pérégrinations d'un ingénieur du XIXe siécle. Actes du Colloque. SABIX **44** (2009), 119–129.

[2] G. Lamé, *Examen de differentes méthodes employées pour résoudre les problèmes de géometrie*, M. V. Courcier imprimeur Libraire, Paris, 1818.

[3] J. Gielis, S. Haesen, L. Verstraelen, Universal shapes: from the supereggs of Piet Hein to the cosmic egg of George Lemaître, *Kragujevac Journal of Mathematics*, **28** (2005), 55–67.

The Laplacian in stretched polar co-ordinates and Applications

by **Pierpaolo Natalini** $^{(*)}$ and **Paolo E. Ricci** $^{(\dagger)}$

$^{(*)}$ *Università degli Studi Roma Tre, Dipartimento di Matematica, Largo San Leonardo Murialdo, 1, 00146 - Roma, Italia*

$^{(\dagger)}$ *Università di Roma "La Sapienza", Dipartimento di Matematica, P.le A. Moro, 2, 00185 - Roma, Italia*

Abstract. We consider the Dirichlet problem for the Laplace equation in a normal-polar domain, i.e. a domain which is normal with respect to polar co-ordinates. Such a domain can be interpreted as a non-isotropically stretched unit circle.

We write down explicitly an infinite linear system for finding coefficients of the Fourier expansion representing solution. This system can be derived from an integral equation whose kernel belongs to L^2. Therefore, by F. Riesz' theory, its solution can be approximated by solving a finite dimensional linear system.

The numerical examples, computed by using Mathematica©, confirm our theoretical results, mainly applied in general domains defined by the so called "superformula" due to J. Gielis.

AMS CLASSIFICATION: 35J05, 35J25.
KEY WORDS: Dirichlet problem, Laplace equation.

1 Introduction

Many applications of Mathematical Physics and Engineering are connected with the Laplacian, however, the most part of BVPs relevant to the Laplacian are solved in explicit form only for domains with a very special shape, namely intervals, cylinders or domains with special (circular or spherical) symmetries [1].

We consider in this lecture an extension of the classical two-dimensional theory to the case of a normal polar domain, i.e. a domain $\mathcal{D}$, which is normal with respect to the polar co-ordinate system.

$\partial\mathcal{D}$ can be interpreted as an *anisotropically stretched unit circle.*

We introduce in the x, y plane the ordinary polar co-ordinates:

$$x = \rho\,\cos\theta\,, \quad y = \rho\,\sin\theta\,, \tag{1.1}$$

and the polar equation of $\partial\mathcal{D}$

$$\rho = r(\theta)\,, \qquad \big(0 \le \theta \le 2\pi\big)\,, \tag{1.2}$$

where $r(\theta) \in C^2[0, 2\pi]$. We suppose the domain $\mathcal{D}$ satisfies

$$0 < A \le \rho \le r(\theta)$$

and therefore $\min_{\theta\in[0,2\pi]} r(\theta) > 0$.

We introduce the stretched radius ρ^* such that

$$\rho = \rho^*\, r(\theta)\,, \tag{1.3}$$

and the curvilinear (i.e. stretched) co-ordinates ρ^*, θ, in the plane x, y,

$$x = \rho^* \, r(\theta) \, \cos\theta \, , \quad y = \rho^* \, r(\theta) \, \sin\theta \, . \tag{1.4}$$

Therefore, $\mathcal{D}$ is obtained assuming $0 \le \theta \le 2\pi$, $0 \le \rho^* \le 1$.

We show how to modify some classical formulas, and we derive methods to compute the coefficients of Fourier-type expansions representing solutions of some classical problems. Of course, this theory can be easily generalized considering weakened hypotheses on the boundary or initial data.

The case of the unit circle is recovered assuming $\rho^* = \rho$ and $r(\theta) \equiv 1$.

2 The Laplacian in stretched polar co-ordinates

We consider a $C^2(\overset{\circ}{\mathcal{D}})$ function $u(x,y) = u(\rho\cos\theta, \rho\sin\theta) = U(\rho,\theta)$ and the Laplace operator in polar co-ordinates

$$\Delta_2 u := \frac{\partial^2 u}{\partial x^2} + \frac{\partial^2 u}{\partial y^2} = \frac{\partial^2 U}{\partial \rho^2} + \frac{1}{\rho}\frac{\partial U}{\partial \rho} + \frac{1}{\rho^2}\frac{\partial^2 U}{\partial \theta^2} \, . \tag{2.1}$$

We start representing this operator in the new stretched co-ordinate system ρ^*, θ.

Putting

$$V(\rho^*, \theta) = u\left[\rho^* r(\theta)\cos\theta, \, \rho^* r(\theta)\sin\theta\right] = U(\rho,\theta) \, ,$$

we find

$$\frac{\partial U}{\partial \rho} = \frac{1}{r(\theta)} \frac{\partial V}{\partial \rho^*} \, , \tag{2.2}$$

$$\frac{\partial^2 U}{\partial \rho^2} = \frac{1}{r^2(\theta)} \frac{\partial^2 V}{\partial \rho^{*2}} \, , \tag{2.3}$$

$$\frac{\partial U}{\partial \theta} = -\rho^* \frac{r'(\theta)}{r(\theta)} \frac{\partial V}{\partial \rho^*} + \frac{\partial V}{\partial \theta} \, , \tag{2.4}$$

$$\begin{aligned} \frac{\partial^2 U}{\partial \theta^2} = {} & \rho^* \, \frac{2r'^2(\theta) - r(\theta)r''(\theta)}{r^2(\theta)} \frac{\partial V}{\partial \rho^*} + \rho^{*2} \, \frac{r'^2(\theta)}{r^2(\theta)} \frac{\partial^2 V}{\partial \rho^{*2}} \\ & - 2\rho^* \, \frac{r'(\theta)}{r(\theta)} \frac{\partial^2 V}{\partial \rho^* \partial \theta} + \frac{\partial^2 V}{\partial \theta^2} \, . \end{aligned} \tag{2.5}$$

Substituting we find our result, i.e.

$$\begin{aligned} \Delta_2 u = {} & \frac{\partial^2 U}{\partial \rho^2} + \frac{1}{\rho}\frac{\partial U}{\partial \rho} + \frac{1}{\rho^2}\frac{\partial^2 U}{\partial \theta^2} \\ = {} & \frac{1}{r^2(\theta)}\left[1 + \frac{r'^2(\theta)}{r^2(\theta)}\right]\frac{\partial^2 V}{\partial \rho^{*2}} + \frac{1}{\rho^* r^2(\theta)}\left[1 + \frac{2r'^2(\theta) - r(\theta)r''(\theta)}{r^2(\theta)}\right]\frac{\partial V}{\partial \rho^*} \\ & - 2\frac{r'(\theta)}{\rho^* r^3(\theta)}\frac{\partial^2 V}{\partial \rho^* \partial \theta} + \frac{1}{\rho^{*2} r^2(\theta)}\frac{\partial^2 V}{\partial \theta^2} \, . \end{aligned} \tag{2.6}$$

For $\rho^* = \rho$, $r(\theta) \equiv 1$, we recover the Laplacian in polar co-ordinates.

3 An equivalent formulation

For further computations, it is more easy to change the polar equation of $\partial\mathcal{D}$ putting

$$\rho = r(\theta) = \frac{1}{R(\theta)}\,, \qquad (0 \leq \theta \leq 2\pi). \tag{3.1}$$

The unit circle is recovered again by putting $R(\theta) \equiv 1$.

Using this polar equation, the corresponding stretched co-ordinates ρ^*, θ, in the plane x, y, are given by

$$x = \rho^* \cos\theta / R(\theta)\,, \quad y = \rho^* \sin\theta / R(\theta)\,, \tag{3.2}$$

and assuming

$$V(\rho^*, \theta) = u\left[\rho^* \cos\theta/R(\theta),\, \rho^* \sin\theta/R(\theta)\right],$$

the Laplacian becomes:

$$\begin{aligned}\Delta_2 u = {} & \left[R^2(\theta) + R'^2(\theta)\right] \frac{\partial^2 V}{\partial \rho^{*2}} + \frac{2}{\rho^*} R(\theta) R'(\theta) \frac{\partial^2 V}{\partial \rho^* \partial\theta} \\ & + \frac{1}{\rho^*} \left[R^2(\theta) + R(\theta) R''(\theta)\right] \frac{\partial V}{\partial \rho^*} + \frac{1}{\rho^{*2}} R^2(\theta) \frac{\partial^2 V}{\partial \theta^2}\,.\end{aligned} \tag{3.3}$$

For $\rho^* = \rho\,,\ R(\theta) \equiv 1,$ we find again the Laplacian in polar co-ordinates.

4 Applications to the Dirichlet problem

Consider the Dirichlet problem for the Laplace equation

$$\begin{cases} \dfrac{\partial^2 u}{\partial x^2} + \dfrac{\partial^2 u}{\partial y^2} = 0\,, & \text{in} \quad \mathring{\mathcal{D}}\,, \\ \\ u = f(x, y) & \text{on} \quad \partial\mathcal{D}\,. \end{cases} \tag{4.1}$$

We prove the following result

Theorem 4.1. – *Putting*

$$u(x, y) = u(\rho\cos\theta, \rho\sin\theta) = U(\rho, \theta)\,,$$

$$F(\theta) = f\left[r(\theta)\cos\theta, r(\theta)\sin\theta\right] = \frac{\alpha_0}{2} + \sum_{m=0}^{\infty} (\alpha_m \cos m\theta + \beta_m \sin m\theta)\ ,$$

the solution of the internal Dirichlet problem *can be represented as*

$$U(\rho, \theta) = \sum_{m=0}^{\infty} (a_m \cos m\theta + b_m \sin m\theta)\, \rho^m\,, \tag{4.2}$$

where $a_0 = \alpha_0/2$, *and the coefficients* $a_m, b_m, (m = 1, 2, 3, \ldots)$ *are given by solving the infinite system*

$$\begin{cases} \displaystyle\sum_{m=1}^{\infty} a_m \int_0^{2\pi} [r(\theta)]^m \cos m\theta \cos h\theta \, d\theta + \sum_{m=1}^{\infty} b_m \int_0^{2\pi} [r(\theta)]^m \sin m\theta \cos h\theta \, d\theta = \pi\alpha_h \,, \\ \displaystyle\sum_{m=1}^{\infty} a_m \int_0^{2\pi} [r(\theta)]^m \cos m\theta \sin h\theta \, d\theta + \sum_{m=1}^{\infty} b_m \int_0^{2\pi} [r(\theta)]^m \sin m\theta \sin h\theta \, d\theta = \pi\beta_h \,, \end{cases}$$

$$(h = 1, 2, 3, \ldots) \,. \tag{4.3}$$

Proof – Putting $\rho^* = \rho \, R(\theta)$,

$$u(\rho\cos\theta, \rho\sin\theta) = U(\rho, \theta) = U\,[\rho^*/R(\theta), \theta] = V(\rho^*, \theta) \,,$$

i.e. using the normal polar co-ordinates, the problem becomes

$$\begin{cases} \left[R^2(\theta) + R'^2(\theta)\right] \dfrac{\partial^2 V}{\partial \rho^{*2}} + \dfrac{2}{\rho^*} \, R(\theta) R'(\theta) \dfrac{\partial^2 V}{\partial \rho^* \partial \theta} \\ \qquad + \dfrac{1}{\rho^*} \, \left[R^2(\theta) + R(\theta) R''(\theta)\right] \dfrac{\partial V}{\partial \rho^*} + \dfrac{1}{\rho^{*2}} \, R^2(\theta) \dfrac{\partial^2 V}{\partial \theta^2} = 0 \,, \\ F(\theta) = V(1, \theta) = f\,[r(\theta)\cos\theta, r(\theta)\sin\theta] \,. \end{cases} \tag{4.4}$$

Searching for a solution of the form

$$U\left(\frac{\rho^*}{R(\theta)}, \theta\right) = P\left(\frac{\rho^*}{R(\theta)}\right) \, \Theta(\theta) = P(\rho) \, \Theta(\theta) \,, \tag{4.5}$$

we find the equation

$$\rho^2 P''(\rho) \, \Theta(\theta) + \rho P'(\rho) \, \Theta(\theta) = - \, P(\rho) \, \Theta''(\theta) \,, \tag{4.6}$$

and therefore

$$\begin{cases} \rho^2 P''(\rho) + \rho P'(\rho) - \lambda^2 P(\rho) = 0 \\ \Theta''(\theta) + \lambda^2 \Theta(\theta) = 0 \,. \end{cases} \tag{4.7}$$

Since

$$\Theta(\theta) = c_1 \cos\lambda\theta + c_2 \sin\lambda\theta \tag{4.8}$$

it follows for periodicity $\lambda = m$ (integer number), and consequently

$$\begin{cases} \Theta(\theta) = c_1 \cos m\theta + c_2 \sin m\theta \\ P(\rho) = d_1 \rho^m + d_2 \rho^{-m} \end{cases} \tag{4.9}$$

so that we have found elementary solutions

$$U(\rho,\theta) = (c_1 \cos m\theta + c_2 \sin m\theta)\,(d_1 \rho^m + d_2 \rho^{-m}) \qquad (m = 0, 1, 2, \dots)\,. \tag{4.10}$$

For the *internal problem*, we must put for a bounded solution: $d_2 = 0$, then

$$U(\rho,\theta) = \sum_{m=0}^{\infty} (a_m \cos m\theta + b_m \sin m\theta)\,\rho^m\,. \tag{4.11}$$

The coefficients $a_m,\, b_m$ are determined by imposing the boundary condition, i.e. assuming $\rho^* = 1$ and therefore putting $\rho = r(\theta)$:

$$f\,[r(\theta)\cos\theta, r(\theta)\sin\theta] = V(1,\theta) = \sum_{m=0}^{\infty} [r(\theta)]^m\,(a_m \cos m\theta + b_m \sin m\theta)\,, \tag{4.12}$$

so that, by using the Fourier method, they are determined by solving the system (4.3).

Remark 1. Note that the system (4.3), assuming the unessential condition $r(\theta) \leq M < 1,\ \forall\theta \in [0, 2\pi]$, can be solved in an approximate way by considering the corresponding finite system where $m = 1, 2, \dots, N$, and $h = 2, \dots, N$, and the solution is convergent when $N \to +\infty$, since it is related to the solution of a compact vectorial integral operator with an L^2 kernel [2]. In fact, substituting the discrete index m with a continuous parameter τ and putting $a_m = a(\tau)$, $b_m = b(\tau)$, $A(\tau) = [a(\tau), b(\tau)]^T$ and similarly $S(\tau,\theta) = [\cos(\tau\theta), \sin(\tau\theta)]^T$, the system (4.3) becomes

$$\int_0^{+\infty} [r(\theta)]^\tau S(\tau,\theta)\cdot A(\tau)d\tau = F(\theta)\,.$$

Assuming $r(\theta) \leq M < 1$, we find

$$\int_0^{\infty}\int_0^{2\pi} |[r(\theta)]^\tau S(\tau,\theta)|^2\, d\tau d\theta < 2\pi \int_0^{+\infty} M^{2\tau} d\tau = \frac{\pi}{\log(1/M)}\,,$$

so that the kernel belongs to L^2.

The compactness of the above mentioned operator can be proved as follows.

Consider the internal Dirichlet problem for the unit circle corresponding to the same function $F(\theta) = f\,[r(\theta)\cos\theta, r(\theta)\sin\theta] = \dfrac{\alpha_0}{2} + \sum_{m=0}^{\infty} (\alpha_m \cos m\theta + \beta_m \sin m\theta)$, considered on the unit circle. The solution of this associated problem is given by

$$\frac{\alpha_0}{2} + \sum_{m=1}^{\infty} (\alpha_m \cos m\theta + \beta_m \sin m\theta)\,\rho^m\,,$$

while the solution of our problem on the boundary $\partial\mathcal{D}$ is

$$\sum_{m=0}^{\infty} (a_m \cos m\theta + b_m \sin m\theta)\,[r(t)]^m\,,$$

where the coefficients a_m, b_m are derived by system (4.3).

The assumption $0 < r(\theta) \le M < 1$ implies that the solution of our problem is dominated by the solution of the associated problem. This is a consequence of the maximum principle.

Therefore,

$$\left|\sum_{m=0}^{\infty} (a_m \cos m\theta + b_m \sin m\theta)\, [r(t)]^m\right| \le \left|\frac{\alpha_0}{2} + \sum_{m=1}^{\infty} (\alpha_m \cos m\theta + \beta_m \sin m\theta)\right|$$

and, by using the linearity of the operator, we find: $|a_0 \le \alpha_0/2|$ and

$$\forall m \ge 1, \qquad |a_m|[r(\theta)]^m \le |\alpha_m|\,, \qquad |b_m|[r(\theta)]^m \le |\beta_m|\,.$$

By Lebesgue's theorem the Fourier coefficients α_m, β_m go to zero when $m \to \infty$ and the order of convergence to zero increases if we increase the regularity property of the function $F(\theta)$. According to the last inequalities, even the coefficients a_m, b_m are infinitesimal (since $r(\theta)$ is bounded), and their order cannot be higher with respect to the order of α_m, β_m. This means that the vectorial operator defined by the system (4.3) is compact. In fact we can split up this operator in the sum of two parts, such that one of them is finite-dimensional and the maximum (or L^2) norm of the other is as small as we wish.

In a similar way the *external problem* can be treated.

4.1 Numerical examples

In the first four examples we consider a general polar equation of the type

$$r(\theta) = \left[c\left(\left|\frac{\cos\left(\frac{1}{2}m\pi\theta\right)}{\alpha}\right|^{n_2} + \left|\frac{\sin\left(\frac{1}{2}m\pi\theta\right)}{\beta}\right|^{n_3}\right)\right]^{-1/n_1}, \qquad \theta \in [0,1] \tag{4.13}$$

introduced by J. Gielis, [3].

In numerical experiments, computed by using Mathematica©, we assume different values of the six parameters $\alpha, \beta, m; n_1, n_2, n_3,$ obtaining very different shapes for the polar domain, including ellipse, Lamé curves (also called *Superellipse*), ovals, m-fold symmetric figures, and so on. We introduced furthermore an extra parameter $c,$ in order to ensure the convergence condition $\max_{\theta\in[0,2\pi]} r(\theta) \le M < 1\,.$ It was noticed in [3] that many characteristic forms occurring in Nature (starfish, equisetum, raspberry, and so on) can be obtained in such a way. We emphasize that almost all two dimensional normal-polar domains are described (or at least approximated as close as we need) by the above mentioned curves.

In the last example we consider the polar equation of the astroid

$$r(\theta) = \frac{|\sec(2\pi\theta)|}{\sqrt{\left(1 + \sqrt[3]{\tan^2(2\pi\theta)}\right)^3}}, \qquad \theta \in [0,1]. \tag{4.14}$$

4.1.1 Example 1

By assuming in (4.13) $c = 2,\ \alpha = 1,\ \beta = 2,\ m = 2;\ n_1 = n_3 = 6,\ n_2 = 2$, we obtain the following shape of the relevant domain $\mathcal{D}$

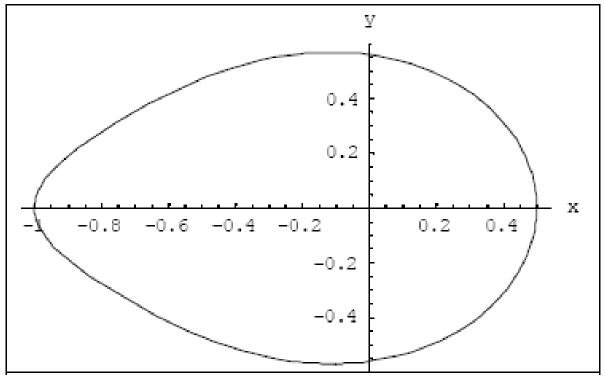

Fig. 1

Let $f(x, y) = x^3y^2 + 30x^2y - 2xy^3$ be the function representing boundary values. Then we obtain the results reported in the following table

$\left\Vert f - u_1 \right\Vert_{L_2} = 4.0099861263$	$\left\Vert \Delta u_1 \right\Vert_{L_2} = 0.\times 10^{-17}$
$\left\Vert f - u_2 \right\Vert_{L_2} = 3.2844400898$	$\left\Vert \Delta u_2 \right\Vert_{L_2} = 0.\times 10^{-17}$
$\left\Vert f - u_3 \right\Vert_{L_2} = 0.00199543982$	
$\left\Vert f - u_4 \right\Vert_{L_2} = 0.00164771835$	
$\left\Vert f - u_5 \right\Vert_{L_2} = 0.000220789634$	
$\left\Vert f - u_6 \right\Vert_{L_2} = 0.000018164343$	
$\left\Vert f - u_7 \right\Vert_{L_2} = 3.646882\times 10^{-6}$	
$\left\Vert f - u_8 \right\Vert_{L_2} = 3.589930\times 10^{-6}$	

Tab. 1. $L^2(\partial\mathcal{D})$ norm of the boundary error f - u_h, where u_h denotes the $(2h+1)$-th partial sum of approximating Fourier series, and $L^2(\mathcal{D})$ norm of the inside error, i.e. the $L^2(\mathcal{D})$ norm-distance from zero of Δu_h.

The following graphs show us the convergence (in general a.e.) of the approximating sequence of functions u_h (dashed line) to the function f (solid line)

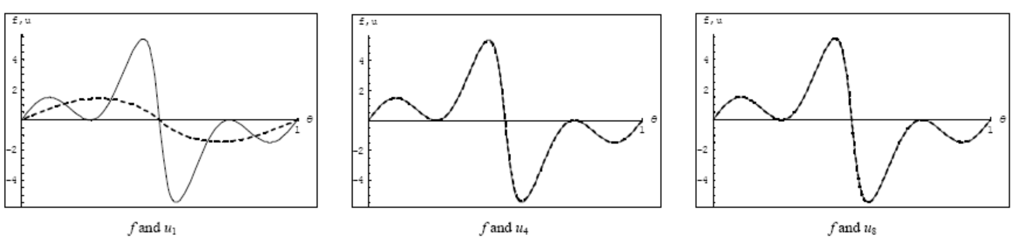
Fig. 2

4.1.2 Example 2

By assuming in (4.13) $c = 8,\ \alpha = 3,\ \beta = 5,\ m = 2;\ n_1 = n_3 = 8,\ n_2 = 2$, we obtain the following shape of the relevant domain $\mathcal{D}$

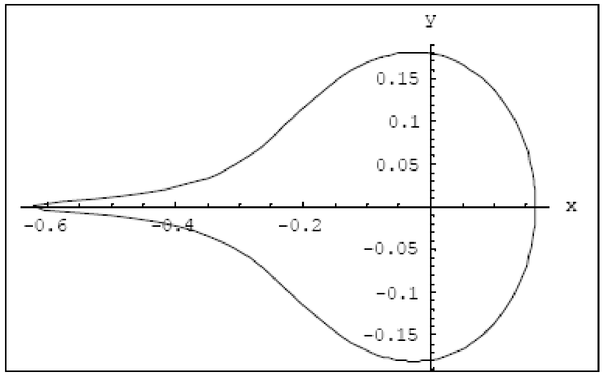

Fig. 3

Let $f(x,y) = \sinh(xy) + \log(x^2 + y^2 + 1)$ be the function representing boundary values. Then we obtain the results reported in the following table

$\left\Vert f - u_1 \right\Vert_{L_2} = 5.86019 \times 10^{-4}$	$\left\Vert \Delta u_1 \right\Vert_{L_2} = 0. \times 10^{-18}$
$\left\Vert f - u_3 \right\Vert_{L_2} = 1.01408 \times 10^{-4}$	$\left\Vert \Delta u_2 \right\Vert_{L_2} = 0. \times 10^{-18}$
$\left\Vert f - u_4 \right\Vert_{L_2} = 4.76476 \times 10^{-5}$	
$\left\Vert f - u_8 \right\Vert_{L_2} = 3.79609 \times 10^{-5}$	

Tab. 2. $L^2(\partial\mathcal{D})$ norm of the boundary error $f - u_h$, where u_h denotes the $(2h+1)$-th partial sum of approximating Fourier series, and $L^2(\mathcal{D})$ norm of the inside error, i.e. the $L^2(\mathcal{D})$ norm-distance from zero of Δu_h.

The following graphs show us the convergence (in general a.e.) of the approximating sequence of functions u_h (dashed line) to the function f (solid line)

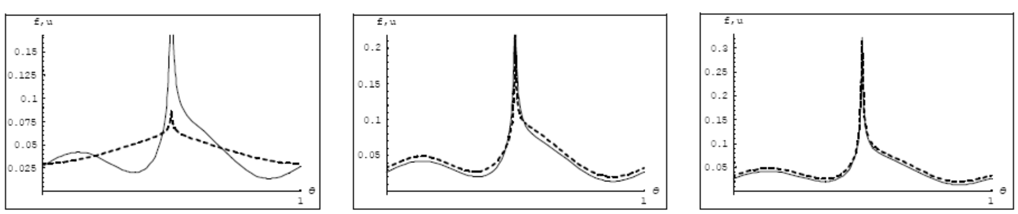

f and u_1 $\quad$ f and u_3 $\quad$ f and u_8

Fig. 4

4.1.3 Example 3

By assuming in (4.13) $c = 22,\ \alpha = 5,\ \beta = 8,\ m = 10;\ n_1 = n_3 = 6,\ n_2 = 4$, we obtain the following shape of the relevant domain $\mathcal{D}$

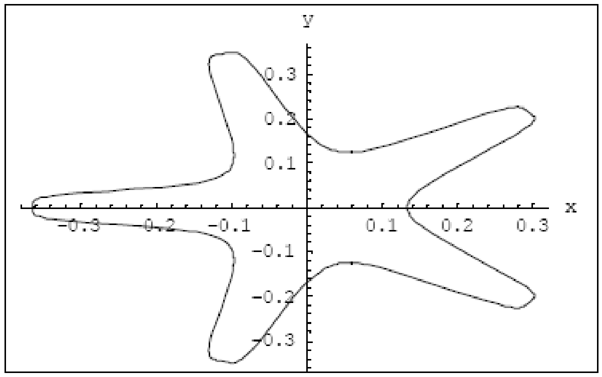

Fig. 5

Let $f(x, y) = \cosh(x + y) + 5x^2y$ be the function representing boundary values. Then we obtain the results reported in the following table

$\left\Vert f - u_1 \right\Vert_{L_2} = 0.000335952$	$\left\Vert \Delta u_1 \right\Vert_{L_2} = 0.\times 10^{-17}$
$\left\Vert f - u_2 \right\Vert_{L_2} = 0.000133587$	$\left\Vert \Delta u_2 \right\Vert_{L_2} = 0.\times 10^{-17}$
$\left\Vert f - u_3 \right\Vert_{L_2} = 0.000101291$	
$\left\Vert f - u_4 \right\Vert_{L_2} = 9.025\times 10^{-5}$	
$\left\Vert f - u_5 \right\Vert_{L_2} = 5.42434\times 10^{-5}$	
$\left\Vert f - u_6 \right\Vert_{L_2} = 4.75581\times 10^{-5}$	
$\left\Vert f - u_7 \right\Vert_{L_2} = 4.75567\times 10^{-5}$	
$\left\Vert f - u_8 \right\Vert_{L_2} = 4.75565\times 10^{-5}$	

Tab. 3. $L^2(\partial\mathcal{D})$ norm of the boundary error $f - u_h$, where u_h denotes the $(2h+1)$-th partial sum of approximating Fourier series, and $L^2(\mathcal{D})$ norm of the inside error, i.e. the $L^2(\mathcal{D})$ norm-distance from zero of Δu_h.

The following graphs show us the convergence (in general a.e.) of the approximating sequence of functions u_h (dashed line) to the function f (solid line)

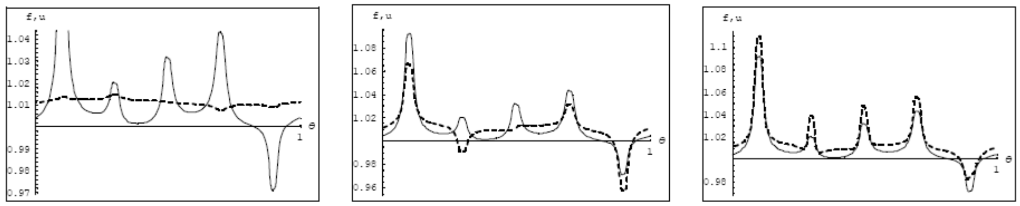

f and u_1 f and u_4 f and u_8

Fig. 6

4.1.4 Example 4

By assuming in (4.13) $c = 22,\ \alpha = 3,\ \beta = 9,\ m = 12;\ n_1 = n_3 = 8,\ n_2 = 2$, we obtain the following shape of the relevant domain $\mathcal{D}$

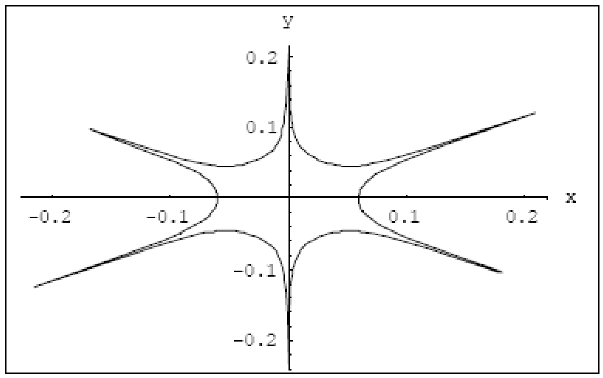

Fig. 7

Let $f(x, y) = 500x^3y^2 + 100x^2y + 2xy^3$ be the function representing boundary values. Then we obtain the results reported in the following table

$\left\Vert f - u_1 \right\Vert_{L_2} = 0.000261555624$	$\left\Vert \Delta u_1 \right\Vert_{L_2} = 0.\times 10^{-18}$
$\left\Vert f - u_3 \right\Vert_{L_2} = 0.000037793595$	$\left\Vert \Delta u_2 \right\Vert_{L_2} = 0.\times 10^{-18}$
$\left\Vert f - u_5 \right\Vert_{L_2} = 0.000016216871$	
$\left\Vert f - u_7 \right\Vert_{L_2} = 7.84024080\times 10^{-6}$	
$\left\Vert f - u_8 \right\Vert_{L_2} = 2.845148588\times 10^{-6}$	

Tab. 4. $L^2(\partial\mathcal{D})$ norm of the boundary error f - u_h, where u_h denotes the ($2h$+1)-th partial sum of approximating Fourier series, and $L^2(\mathcal{D})$ norm of the inside error, i.e. the $L^2(\mathcal{D})$ norm-distance from zero of Δu_h.

The following graphs show us the convergence (in general a.e.) of the approximating sequence of functions u_h (dashed line) to the function f (solid line)

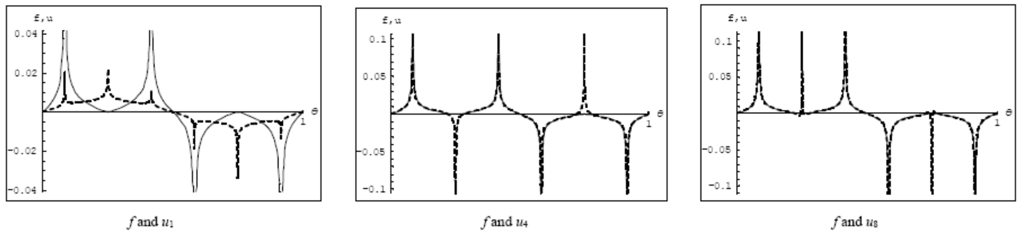

Fig. 8

4.1.5 Example 5

The shape of the domain $\mathcal{D}$ relating to the polar equation (4.14) is the following

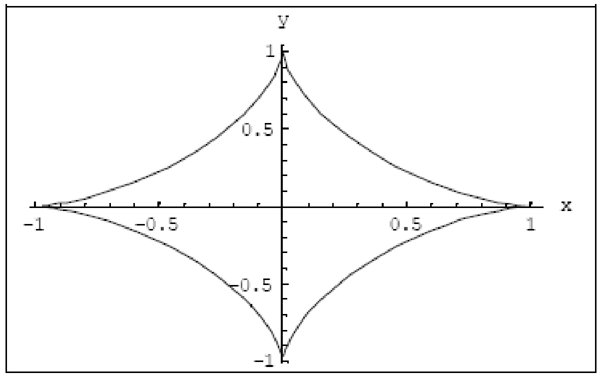

Fig. 9

Here we consider two cases. In the first case we assume $f(x,y) = e^{xy^2}/2 + 10x^3y$ as the function representing boundary values. Then we obtain the results reported in the following table

$\|f-u_2\|_{L_2} = 0.0134478$	$\|\Delta u_1\|_{L_2} = 0.\times 10^{-16}$
$\|f-u_4\|_{L_2} = 0.00195702$	$\|\Delta u_2\|_{L_2} = 0.\times 10^{-16}$
$\|f-u_8\|_{L_2} = 2.2544\times 10^{-5}$	

Tab. 5. $L^2(\partial\mathcal{D})$ norm of the boundary error f - u_h, where u_h denotes the $(2h+1)$-th partial sum of approximating Fourier series, and $L^2(\mathcal{D})$ norm of the inside error, i.e. the $L^2(\mathcal{D})$ norm-distance from zero of Δu_h.

The following graphs show us the convergence (in general a.e.) of the approximating sequence of functions u_h (dashed line) to the function f (solid line)

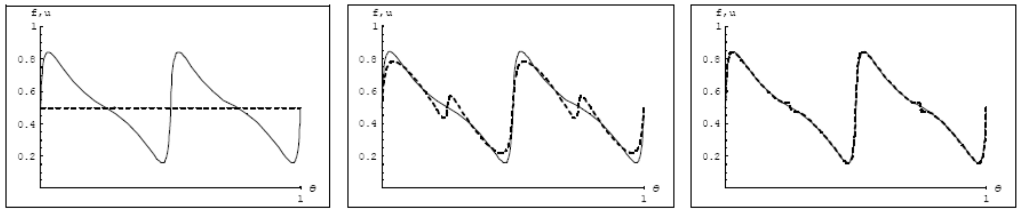

f and u_2 f and u_4 f and u_{12}

Fig. 10

In the second case we assume $f(x, y) = 40x^3y + 50x^2y^3$ as the function representing boundary values. Then we obtain the results reported in the following table

$\lVert f - u_1 \rVert_{L_2} = 0.640604$	$\lVert \Delta u_1 \rVert_{L_2} = 0.\times 10^{-16}$
$\lVert f - u_6 \rVert_{L_2} = 0.00544712$	$\lVert \Delta u_2 \rVert_{L_2} = 0.\times 10^{-16}$
$\lVert f - u_{12} \rVert_{L_2} = 2.96858\times 10^{-5}$	

Tab. 6. $L^2(\partial\mathcal{D})$ norm of the boundary error f - u_h, where u_h denotes the $(2h+1)$-th partial sum of approximating Fourier series, and $L^2(\mathcal{D})$ norm of the inside error, i.e. the $L^2(\mathcal{D})$ norm-distance from zero of Δu_h.

The following graphs show us the convergence (in general a.e.) of the approximating sequence of functions u_h (dashed line) to the function f (solid line)

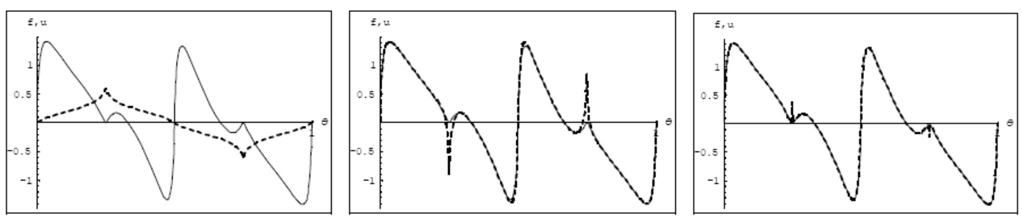

f and u_1 f and u_6 f and u_{12}

Fig. 11

Remark 2. We note that when the boundary values have wide oscillations, it is necessary to increase the number N of terms in the relevant Fourier expansion, in order to obtain better results.

Remark 3. The L^2 norm of the difference between the exact solution and its approximate values is always vanishing in the interior of the considered domain, and generally small on the boundary. Point-wise convergence seems to be true on the whole boundary, with only exception of a set of measure zero, corresponding to cusped or quasi-cusped points. In these points oscillations of the approximate solution, recalling the classical Gibbs phenomenon, usually appear.

Remark 4. It seems that our numerical experiments confirm the outstanding results by Lennart Carleson, the winner of 2006 Abel Prize, about the almost-everywhere point-wise convergence of Fourier series [4].

5 Conclusion

It seems that the use of the normal polar co-ordinates will allow us to find close formulas for a wide set of classical problems, avoiding the use of conformal mappings [5]. A comparison with the conformal mapping technique is in progress.

In forthcoming articles [6]- [7] we show that the above technique can be applied to solve classical problems of a vibrating membrane and heat equation relevant to normal-polar shaped domains.

Similar methods can also be used for particular sets of three-dimensional domains, and numerical computations will be presented soon, in order to confirm our results.

Acknowledgments. Useful discussions with Prof. Dr. George Jaiani of the Tbilisi State University are gratefully recognized.

References

[1] L.C. Andrews, *Special functions of Mathematics for Engineers*, Oxford Univ. Press, Oxford - New York, 1998.

[2] F. Riesz, *Les systèmes d'équations linéaires à une infinité d'inconnues*, Gauthier Villars, Paris, 1952.

[3] J. Gielis, A Generic geometric transformation that unifies a wide range of natural and abstract shapes, *Amer. J. Botany*, **90**, (2003), 333–338.

[4] L. Carleson, On convergence and growth of partial sums of Fourier series. *Acta Math.*, **116** (1966), 135–157.

[5] G. Fichera, L. De Vito. *Funzioni analitiche di una variabile complessa*, Veschi, Roma, 1964.

[6] P. Natalini, R. Patrizi, P.E. Ricci, Free vibrations of a normal-polar shaped membrane, (submitted).

[7] P. Natalini, R. Patrizi, P.E. Ricci, Heat problems for a normal-polar shaped body, (submitted).

Solution of the Dirichlet problem for the Laplace equation in a general cylinder

by **Diego Caratelli** $^{(\star)}$, **Bruna Germano** $^{(\circ)}$,

Matthew X. He $^{(*)}$ and **Paolo E. Ricci** $^{(\dagger)}$

$^{(\star)}$ *Delft University of Technology*
Mekelweg, 4 - 2628 CD, Delft, the Netherlands

$^{(\circ)}$ *Università di Roma "La Sapienza", Dipartimento DMMM*
Via A. Scarpa, 14, 00161 - Roma, Italia

$^{(*)}$ *Nova Southeastern University*
3301 College Avenue, Ft Lauderdale, FL 33314-7796 U.S.A.

$^{(\dagger)}$ *Università di Roma "La Sapienza", Dipartimento di Matematica*
P.le A. Moro, 2, 00185 - Roma, Italia

Abstract. We consider the Dirichlet problem for the Laplace equation in a bounded cylindrical domain $\mathcal{C} := \mathcal{D} \times [0,1]$, where $\mathcal{D}$ is a starlike domain of the (x,y)-plane. We show how to construct the solution by using the Fourier series method. We derive some numerical results defining $\partial\mathcal{D}$ by means of the so called "superformula" introduced by J. Gielis. By using a computer algebra system we find a quite rapid convergence of the approximate solutions to the real one, with only possible exceptions corresponding to singular points in which oscillations recalling Gibbs' phenomenon appear. Our findings are in agreement with the theoretical results on Fourier series due to L. Carleson.

AMS CLASSIFICATION: 35J05, 35J25.

KEY WORDS: Dirichlet problem, Laplace equation, starlike domain, Fourier series.

1 Introduction

In recent articles [1], [2] it was shown that for a plane starlike domain (even lying on a two fold Riemann surface) the Dirichlet problem for the Laplace equation can be solved in explicit form without using conformal mappings. Therefore, computation of approximate solutions can be obtained by using symbolic computer algebra programs, avoiding the finite difference methods.

Different techniques were used in literature for solving this classical problem in general domains, both from the theoretical and numerical point of view (see e.g. [5], representing solution by using boundary layer techniques; [6], comparing several numerical methods; [7] , solving by iterative methods the corresponding boundary integral equation; [8], approximating the relevant Green function by the least squares method; [9], using the grid method; [10], considering the system of linear equations arising from an unusual finite difference approximation; [11], solving linear systems relevant to elliptic partial differential equations by relaxation methods). However, none of the above mentioned articles is connected with the approach we consider here, which makes use of simple tools, tracing back to the original Fourier method.

We show in this article an extension of preceding results to the case of a bounded cylinder $\mathcal{C} := \mathcal{D} \times [0,1]$, whose basic line (directrix) $\partial\mathcal{D}$ is the boundary of a starlike domain $\mathcal{D}$, i.e. a domain which is normal with respect to a suitable polar co-ordinate system.

It is worth to note that the technique we developed in [1] can be applied even in the case when the boundary of the considered domain is interlaced [2] (i.e. the polar equation of the boundary $\partial\mathcal{D}$ is of the type $\rho = r(\theta)$, with $0 \leq \theta \leq 4\pi$, and the boundary data are periodic of period 4π). This more general case can be reduced to the classical one by considering the plane as a two-fold Riemann surface, and therefore the relevant data are prescribed even on portion of boundary curves lying inside the considered domain. This recalls the situation of non-local boundary value problems, introduced and first studied by A.V. Bitsadze and A.A. Samarskii [12], and subsequently by many authors (see e.g. [13]).

The boundary of domains we have considered in our last Section are defined by using the so called “superformula” due to J. Gielis [14].

Several numerical examples, computed by using the Computer Algebra system Mathematica©, confirm, even in the considered case, the theoretical results by L. Carleson [15], since we have found a point-wise convergence in all regular points of the boundary, with possible oscillation usually occurring only in singular points (for the function or its derivative).

2 The problem

Let consider a cylindrical domain $\mathcal{C}$ of the $\mathbf{R}^3$ space defined by

$$(x,y) \in \mathcal{D}\,, \quad z \in [0,1]\ ,$$

such that $\mathcal{D}$ is a starlike domain of the (x,y)-plane. We introduce in the plane the ordinary polar co-ordinates:

$$x = \rho\cos\theta\,, \quad y = \rho\sin\theta\,, \tag{2.1}$$

and the polar equation of $\partial\mathcal{D}$

$$\rho = r(\theta) \qquad (0 \leq \theta \leq 2\pi)\,, \tag{2.2}$$

where $r(\theta)$ is a piecewise $C^2[0,2\pi]$ function. We suppose the domain $\mathcal{D}$ satisfies

$$0 < A \leq \rho \leq r(\theta)$$

and therefore $\min_{\theta\in[0,2\pi]} r(\theta) > 0$.

We introduce the stretched radius ϱ^* such that

$$\rho = \varrho^* r(\theta)\ , \tag{2.3}$$

and the curvilinear (i.e. stretched) co-ordinates ϱ^*, θ in the (x,y)-plane

$$x = \varrho^* r(\theta)\cos\theta\,, \quad y = \varrho^* r(\theta)\sin\theta\,. \tag{2.4}$$

Therefore, $\mathcal{D}$ is obtained assuming $0 \leq \theta \leq 2\pi$, $0 \leq \varrho^* \leq 1$, and $\partial\mathcal{D}$ is the basic line (directrix) of the relevant cylindrical surface $\partial\mathcal{D} \times [0,1]$.

We consider in $\mathcal{C}$ the Dirichlet problem for the Laplace equation

$$(P) \quad \begin{cases} \Delta u := \dfrac{\partial^2 u}{\partial x^2} + \dfrac{\partial^2 u}{\partial y^2} + \dfrac{\partial^2 u}{\partial z^2} = 0\,, \quad \text{in} \quad \overset{\circ}{C}\,, \\ u\,(x, y, 0) = f_0\,(x, y)\ , \\ u\,(x, y, 1) = f_1\,(x, y)\ , \\ \ u\,(x, y, z)|_{(x,y)\in\partial\mathcal{D}} = g\,(x, y, z)|_{(x,y)\in\partial\mathcal{D}}\ , \end{cases} \tag{2.5}$$

where $f_0\,, f_1\,, g$ are given L^2 (but actually piecewise continuous) functions.

In order to find the solution, we split the problem into the following two

$$(P_I) \quad \begin{cases} \Delta u_I := \dfrac{\partial^2 u_I}{\partial x^2} + \dfrac{\partial^2 u_I}{\partial y^2} + \dfrac{\partial^2 u_I}{\partial z^2} = 0\ , \quad \text{in} \quad \overset{\circ}{C}\,, \\ u_I\,(x, y, 0) = f_0\,(x, y)\ , \\ u_I\,(x, y, 1) = f_1\,(x, y)\ , \\ \ u_I\,(x, y, z)|_{(x,y)\in\partial\mathcal{D}} = 0\,, \end{cases} \tag{2.6}$$

$$(P_{II}) \quad \begin{cases} \Delta u_{II} := \dfrac{\partial^2 u_{II}}{\partial x^2} + \dfrac{\partial^2 u_{II}}{\partial y^2} + \dfrac{\partial^2 u_{II}}{\partial z^2} = 0\,, \quad \text{in} \quad \overset{\circ}{C}\,, \\ u_{II}\,(x, y, 0) = 0\,, \\ u_{II}\,(x, y, 1) = 0\,, \\ \ u_{II}\,(x, y, z)|_{(x,y)\in\partial\mathcal{D}} = g\,(x, y, z)|_{(x,y)\in\partial\mathcal{D}}\ . \end{cases} \tag{2.7}$$

Therefore, after finding the solutions u_I of problem (P_I) and u_{II} of problem (P_{II}), the solution of problem (P) is given by

$$u\,(x, y, z) = u_I\,(x, y, z) + u_{II}\,(x, y, z)\ . \tag{2.8}$$

3 Solution of problem (P_I)

According to the results in [2], we set

$$\rho = r\,(\theta)\ = \frac{1}{\Upsilon\,(\theta)} \qquad (0 \le \theta \le 2\pi)\,. \tag{3.1}$$

By using this polar equation, the corresponding stretched co-ordinates $\varrho^*\,, \theta$ in the (x, y)-plane are given by

$$x = \varrho^* \cos\theta/\Upsilon\,(\theta)\ , \quad y = \varrho^* \sin\theta/\Upsilon\,(\theta)\ . \tag{3.2}$$

Assuming

$$V\,(\varrho^*, \theta, z) = u\,(\varrho^* \cos\theta/\Upsilon\,(\theta)\,, \varrho^* \sin\theta/\Upsilon\,(\theta)\,, z)\ ,$$

the Laplacian becomes

$$\begin{aligned} \Delta u \quad &= \quad \left[\Upsilon^2\,(\theta) + \Upsilon'^2\,(\theta)\right] \frac{\partial^2 V}{\partial \varrho^{*2}} + \frac{2\Upsilon\,(\theta)\,\Upsilon'\,(\theta)}{\varrho^*} \frac{\partial^2 V}{\partial \varrho^* \partial\theta} \\ &\quad + \frac{\Upsilon^2\,(\theta) + \Upsilon\,(\theta)\,\Upsilon''\,(\theta)}{\varrho^*} \frac{\partial V}{\partial \varrho^*} + \frac{\Upsilon^2\,(\theta)}{\varrho^{*2}} \frac{\partial^2 V}{\partial \theta^2} + \frac{\partial^2 V}{d z^2}\,. \end{aligned} \tag{3.3}$$

For $\varrho^* = \rho\,,\, R(\theta) \equiv 1$ we find again the Laplacian in cylindrical co-ordinates.

We prove the following result

Theorem 3.1. *Set*

$$u(x,y,z) = u(\rho\cos\theta, \rho\sin\theta, z) = U(\rho,\theta,z)\ ,$$

$$\Phi_0(\varrho^*,\theta) = f_0(\varrho^* r(\theta)\cos\theta, \varrho^* r(\theta)\sin\theta) = \sum_{m=0}^{\infty}\left[\alpha_m(\varrho^*)\cos m\theta + \beta_m(\varrho^*)\sin m\theta\right]\ ,$$

$$\Phi_1(\varrho^*,\theta) = f_1(\varrho^* r(\theta)\cos\theta, \varrho^* r(\theta)\sin\theta) = \sum_{m=0}^{\infty}\left[\gamma_m(\varrho^*)\cos m\theta + \delta_m(\varrho^*)\sin m\theta\right]\ ,$$

where $\alpha_m(\varrho^*)\,,\,\beta_m(\varrho^*)$ *and* $\gamma_m(\varrho^*)\,,\,\delta_m(\varrho^*)$ *are the Fourier coefficients of* Φ_0 *and* Φ_1 *as functions of* θ*, for every fixed* ϱ^**. Then, the solution of the* interior Dirichlet problem (P_I) *can be represented as*

$$U_I(\varrho^*,\theta,z) = \sum_{m=0}^{\infty}\sum_{l=1}^{\infty}\Big(A_{m,l}\cosh\zeta_l^{(m)} z\cos m\theta + B_{m,l}\cosh\zeta_l^{(m)} z\sin m\theta$$
$$+ C_{m,l}\sinh\zeta_l^{(m)} z\cos m\theta + D_{m,l}\sinh\zeta_l^{(m)} z\sin m\theta\Big)\cdot J_m\left(\zeta_l^{(m)}\varrho^*\right)\ , \tag{3.4}$$

where $\zeta_l^{(m)}$ *denotes the* $l-$*th positive root of the Bessel function of the first type and order* m*. The coefficients* $A_{m,l}\,,\,B_{m,l}\,,\,C_{m,l}\,,\,D_{m,l}\ (m = 0,1,2,\ldots;\, l = 1,2,3,\ldots)$*, after setting*

$$\left\{\begin{array}{c}\mu_{m,l}\\ \nu_{m,l}\\ \sigma_{m,l}\\ \tau_{m,l}\end{array}\right\} = \frac{2}{J_{m+1}\left(\zeta_l^{(m)}\right)^2}\int_0^1 \varrho^*\left\{\begin{array}{c}\alpha_m(\varrho^*)\\ \beta_m(\varrho^*)\\ \gamma_m(\varrho^*)\\ \delta_m(\varrho^*)\end{array}\right\} J_m\left(\zeta_l^{(m)}\varrho^*\right)\, d\varrho^* \tag{3.5}$$

$$(m = 0,1,2,\ldots\,;\, l = 1,2,3,\ldots)$$

are given by the equations

$$\left\{\begin{array}{l}A_{m,l} = \mu_{m,l}\,,\\[2mm] B_{m,l} = \nu_{m,l}\,,\\[2mm] C_{m,l} = \dfrac{1}{\sinh\zeta_l^{(m)}}\left(\sigma_{m,l} - \mu_{m,l}\cosh\zeta_l^{(m)}\right)\ ,\\[2mm] D_{m,l} = \dfrac{1}{\sinh\zeta_l^{(m)}}\left(\tau_{m,l} - \nu_{m,l}\cosh\zeta_l^{(m)}\right)\end{array}\right. \tag{3.6}$$

$$(m = 0,1,2,\ldots\,;\, l = 1,2,3,\ldots)\,.$$

Proof – Noting that in the stretched co-ordinates for the (x,y)-plane the cylinder $\mathcal{C}$ becomes a cylinder having the unit circle as a directrix, we can use the usual eigenfunction method [16] and separation of variables (with respect to the variables $\varrho^*\,,\,\theta\,,\,z$).

By setting

$$V(\rho,\theta,z) = \mathrm{P}\left(\frac{\rho}{r(\vartheta)}\right)\,\Theta(\theta)\ Z(z)\ ,$$

we find the ordinary differential equations

$$\begin{cases} \Theta'' = -m^2\Theta\,, \quad (m \text{ integral number}) \\ Z'' = \lambda^2 Z\,, \\ \rho^2 \mathrm{P}'' + \rho \mathrm{P}' + \left(\lambda^2\rho^2 - m^2\right)\mathrm{P} = 0\,, \end{cases}$$

whose solutions are given by

$$\begin{cases} \Theta(\theta) = A_m \cos m\theta + B_m \sin m\theta\,, \\ Z(z) = C_\lambda \cosh \lambda z + D_\lambda \sinh \lambda z\,, \\ \mathrm{P}(\rho) = E_{m,\lambda} J_m(\lambda\rho) + F_{m,\lambda} Y_m(\lambda\rho)\,. \end{cases}$$

As usual we have to assume $F_{m,\lambda} = 0$ for the boundedness of the solution. Furthermore, imposing the boundary condition $(2.6)_4$, we find that $\lambda = \zeta_l^{(m)}$, $(l = 1, 2, 3, \dots)$, since it must run over the set of zeros of the Bessel function $J_m(\cdot)$. Therefore the solution of problem (P_I) can be searched in the form

$$U_I(\rho,\theta,z) = \sum_{m=0}^{\infty}\sum_{l=1}^{\infty}\Big(A_{m,l}\cosh\zeta_l^{(m)} z\cos m\theta + B_{m,l}\cosh\zeta_l^{(m)} z\sin m\theta + \\ + C_{m,l}\sinh\zeta_l^{(m)} z\cos m\theta + D_{m,l}\sinh\zeta_l^{(m)} z\sin m\theta\Big)\cdot J_m\left(\frac{\zeta_l^{(m)}\rho}{r(\theta)}\right). \tag{3.7}$$

Imposing conditions $(2.6)_2$, $(2.6)_3$, and using Fourier's method, the equations (3.5)-(3.6) follow. Therefore we find the solution of problem (P_I) in the form reported in equation (3.4).

4 Solution of problem (P_{II})

By using the same notations as before, we prove the following result

Theorem 4.1. *Set*

$$G(\theta,z) = g(r(\theta)\cos\theta, r(\theta)\sin\theta, z) = \sum_{n=1}^{\infty}\psi_n(\theta)\sin n\pi z\,, \tag{4.1}$$

where $\psi_n(\theta)$ are the Fourier sine coefficients of G as function of z, for every fixed θ. Then, the solution of the interior Dirichlet problem (P_{II}) *can be represented as*

$$U_{II}(\varrho^*,\theta,z) = \sum_{m=0}^{\infty}\sum_{n=1}^{\infty} I_m(n\pi\varrho^* r(\theta))\left(\tilde{A}_{m,n}\cos m\theta + \tilde{B}_{m,n}\sin m\theta\right)\sin n\pi z\,, \tag{4.2}$$

where the coefficients $\tilde{A}_{m,n}$, $\tilde{B}_{m,n}$, $(m = 0,1,2,\dots;\ n = 1,2,3,\dots)$ can be derived by solving the infinite linear system

$$\sum_{m=0}^{\infty}\underline{\underline{\Gamma}}_{m,n,k}\cdot\underline{\tilde{X}}_{m,n} = \underline{\Psi}_{n,k} \tag{4.3}$$

$$(n = 1,2,3,\dots;\ k = 0,1,2,\dots)\,,$$

being

$$\underline{\underline{\Gamma}}_{m,n,k} = \int_0^{2\pi} I_m(n\pi r(\theta))\begin{bmatrix}\cos m\theta\cos k\theta & \sin m\theta\cos k\theta \\ \cos m\theta\sin k\theta & \sin m\theta\sin k\theta\end{bmatrix} d\theta\,,$$

$$\underline{\Psi}_{n,k} = \int_0^{2\pi} \psi_n(\theta) \begin{bmatrix} \cos k\theta \\ \sin k\theta \end{bmatrix} d\theta \,,$$

$$\underline{\tilde{X}}_{m,n} = \begin{bmatrix} \tilde{A}_{m,n} \\ \tilde{B}_{m,n} \end{bmatrix}$$

$$(m = 0, 1, 2, \ldots \,;\, n = 1, 2, 3, \ldots \,;\, k = 0, 1, 2, \ldots) \,.$$

Proof – To solve the problem (P_{II}), after separating variables, it is convenient to set

$$\begin{cases} \Theta'' = -m^2 \Theta \,, \quad (m \text{ integral number}) \\ Z'' = -n^2 \pi^2 Z \,, \\ \rho^2 \mathrm{P}'' + \rho \mathrm{P}' - \left(n^2 \pi^2 \rho^2 + m^2 \right) \mathrm{P} = 0 \,, \end{cases}$$

and therefore

$$\begin{cases} \Theta(\theta) = \tilde{A}_m \cos m\theta + \tilde{B}_m \sin m\theta \,, \\ Z(z) = \tilde{C}_n \cos n\pi z + \tilde{D}_n \sin n\pi z \,, \\ \mathrm{P}(\rho) = \tilde{E}_{m,n} I_m(n\pi\rho) + \tilde{F}_{m,n} K_m(n\pi\rho) \,. \end{cases}$$

Assuming again $\tilde{F}_{m,n} = 0$, the solution of problem (P_{II}) can be searched in the form

$$\begin{aligned} U_{II}(\rho, \theta, z) \quad = \quad & \sum_{m=0}^{\infty} \sum_{n=0}^{\infty} I_m(n\pi\rho) \left(\tilde{A}_m \cos m\theta + \tilde{B}_m \sin m\theta \right) \cdot \\ & \cdot \left(\tilde{C}_n \cos n\pi z + \tilde{D}_n \sin n\pi z \right) \,. \end{aligned} \tag{4.4}$$

Imposing conditions $(2.8)_2$-$(2.7)_3$, we find

$$\sum_{m=0}^{\infty} \sum_{n=0}^{\infty} \tilde{C}_n I_m(n\pi\rho) \left(\tilde{A}_m \cos m\theta + \tilde{B}_m \sin m\theta \right) = 0 \qquad \forall (\rho, \theta) \,,$$

and

$$\sum_{m=0}^{\infty} \sum_{n=0}^{\infty} (-1)^n \tilde{C}_n I_m(n\pi\rho) \left(\tilde{A}_m \cos m\theta + \tilde{B}_m \sin m\theta \right) = 0 \qquad \forall (\rho, \theta) \,,$$

respectively. These conditions can be easily satisfied by assuming $\tilde{C}_n = 0$ $(n = 0, 1, 2, \ldots)$, so that the solution is reduced to the form

$$U_{II}(\rho, \theta, z) = \sum_{m=0}^{\infty} \sum_{n=1}^{\infty} I_m(n\pi\rho) \left(\tilde{A}_{m,n} \cos m\theta + \tilde{B}_{m,n} \sin m\theta \right) \sin n\pi z \,. \tag{4.5}$$

Therefore, imposing the condition $(2.7)_4$, recalling (4.1) and using Fourier method, we get our result.

5 Numerical examples

In the following examples we consider for $\partial\mathcal{D}$ a general polar equation of the type

$$r(\theta) = \left(\left| \frac{\cos \frac{m_1 \theta}{4}}{\alpha} \right|^{n_1} + \left| \frac{\sin \frac{m_2 \theta}{4}}{\beta} \right|^{n_2} \right)^{-1/n_3} \tag{5.1}$$

introduced by J. Gielis [14] where, in particular, $\theta \in [0, 2\pi]$ in the first three examples, whereas $\theta \in [0, 4\pi]$ in the last one.

In numerical experiments, computed by using Mathematica©, we make different choice for the seven parameters α, β, m_1, m_2, n_1, n_2, n_3, obtaining very different shapes for the basic polar domain, including ellipse, Lamé curves (also called *Superellipse*), ovals, $m-$fold symmetric figures, and so on. It was noticed in [14] that many characteristic forms occurring in Nature (starfish, equisetum, raspberry, and so on) can be obtained in such a way. We emphasize that almost all two dimensional normal-polar domains are described (or at least approximated as close as we need) by the above mentioned curves, so that the solution of the Dirichlet problem for the Laplace equation relevant to very general cylinders can be approximated in this way.

To assess the performance of the proposed technique in terms of numerical accuracy and convergence rate, the relative boundary error has been evaluated as follows

$$e_{L,M,N} = \frac{\|u_{L,M,N}(x,y,z) - h(x,y,z)\|}{\|h(x,y,z)\|}, \tag{5.2}$$

where $\|\cdot\|$ denotes the usual $L^2(\partial\mathcal{C})$ norm, and

$$h(x,y,z) = \begin{cases} f_0(x,y), & (x,y) \in \mathcal{D}, \quad z = 0, \\ f_1(x,y), & (x,y) \in \mathcal{D}, \quad z = 1, \\ g(x,y,z), & (x,y) \in \partial\mathcal{D}, \quad z \in (0,1), \end{cases}$$

is the function describing the boundary values. In (5.2) $u_{L,M,N}(x,y,z)$ is the Fourier-type expansion of orders L, M, N approximating the solution of the Dirichlet problem for the Laplace equation (2.5), namely

$$u_{L,M,N}(x,y,z) = u_{I_{L,M}}(x,y,z) + u_{II_{M,N}}(x,y,z),$$

being

$$\begin{aligned} u_{I_{L,M}}(x,y,z) &= u_{I_{L,M}}(\rho\cos\theta, \rho\sin\theta, z) = U_{I_{L,M}}(\rho,\theta,z) \\ &= \sum_{m=0}^{M}\sum_{l=1}^{L}\Big(A_{m,l}\cosh\zeta_l^{(m)} z\cos m\theta + B_{m,l}\cosh\zeta_l^{(m)} z\sin m\theta \\ &+ C_{m,l}\sinh\zeta_l^{(m)} z\cos m\theta + D_{m,l}\sinh\zeta_l^{(m)} z\sin m\theta\Big)\cdot J_m\left(\frac{\zeta_l^{(m)}\rho}{r(\theta)}\right), \end{aligned}$$

and

$$\begin{aligned} u_{II_{M,N}}(x,y,z) &= u_{II_{M,N}}(\rho\cos\theta, \rho\sin\theta, z) = U_{II_{M,N}}(\rho,\theta,z) \\ &= \sum_{m=0}^{M}\sum_{n=1}^{N} I_m(n\pi\rho)\left(\tilde{A}_{m,n}\cos m\theta + \tilde{B}_{m,n}\sin m\theta\right)\sin n\pi z, \end{aligned}$$

respectively.

5.1 Example 1

By assuming in (5.1) $\alpha = 1/8$, $\beta = 1$, $m_1 = m_2 = 2$, $n_1 = 2$, $n_2 = n_3 = 6$, and $\theta \in [0, 2\pi]$, the domain $\mathcal{C}$ features the ovaloid-like shape shown in Fig. 1. Let

$N = 8$

$e_{L,M,N}$	$L=1$	$L=4$	$L=8$
$M=0$	91.895%	74.368%	74.307%
$M=5$	61.718%	10.223%	8.918%
$M=10$	61.199%	5.973%	3.112%

(*a*)

$M = 10$

$e_{L,M,N}$	$L=1$	$L=4$	$L=8$
$N=1$	86.085%	60.836%	60.622%
$N=4$	61.228%	6.262%	3.636%
$N=8$	61.199%	5.973%	3.112%

(*b*)

$L = 8$

$e_{L,M,N}$	$M=0$	$M=5$	$M=10$
$N=1$	74.307%	60.770%	60.622%
$N=4$	74.307%	8.198%	3.636%
$N=8$	74.307%	8.918%	3.112%

(*c*)

Table 1: Relative boundary error $e_{L,M,N}$ for different expansion orders of the Fourier-like solution of the Dirichlet problem for the Laplace equation (2.5) in a cylindrical domain $\mathcal{C}$, whose directrix is described by the polar equation (5.1) with parameters $\alpha = 1/8$, $\beta = 1$, $m_1 = m_2 = 2$, $n_1 = 2$, $n_2 = n_3 = 6$.

$f_0(x,y) = \left(1 - x^2 - 2y^2\right)/5$, $f_1(x,y) = e^{-7\left(x^2+y^2\right)}\cos(9x+5y)$, and $g(x,y,z) = 4xy\log\left(1 + x^2 + 2y^2 + 3z^2\right)\sin(3\pi z)$ be the functions describing the boundary values. Then, as regards the relative boundary error $e_{L,M,N}$, the numerical results summarized in Table 1 are obtained. Finally, the maps in Fig. 1 clearly show the convergence of the approximating sequence of functions $u_{L,M,N}(x,y,z)$ to the boundary values $h(x,y,z)$.

5.2 Example 2

By assuming in (5.1) $\alpha = \beta = 3/4$, $m_1 = m_2 = 5$, $n_1 = n_2 = 7$, $n_3 = 2$, and $\theta \in [0, 2\pi]$, the domain $\mathcal{C}$ features the starfish-like shape shown in Fig. 2. Let $f_0(x,y) = 1 + 2x^2 + 3y^2$, $f_1(x,y) = 17\,x\,y\,\mathrm{sech}\left(1 + 7x^2\right)\sin(x+2y)/\left(1 + 3y^2 + 5y^4\right)$, and $g(x,y,z) = x^3z + xyz + y^2z + z^2 - x^3z^2 - xyz^2 - y^2z^2 - z^3$ be the functions describing the boundary values. Then, as regards the relative boundary error $e_{L,M,N}$, the numerical results summarized in Table 2 are obtained. Finally, the maps in Fig. 2 clearly show the convergence of the approximating sequence of functions $u_{L,M,N}(x,y,z)$ to the boundary values $h(x,y,z)$.

5.3 Example 3

By assuming in (5.1) $\alpha = \beta = 1/8$, $m_1 = 5$, $m_2 = 7$, $n_1 = n_2 = 5$, $n_3 = 17$, and $\theta \in [0, 2\pi]$, the domain $\mathcal{C}$ features the shape shown in Fig. 3. Let $f_0(x,y) = 4e^x - 5y^3 + 6y$, $f_1(x,y) = 17\sin\left(5xy^2 + 3x^2y\right)$, and $g(x,y,z) = 5(x - \cos\pi y + \sin\pi z)/\left(2 - 5z + 6z^2\right)$ be the functions describing the boundary values. Then, as regards the relative boundary error $e_{L,M,N}$, the numerical results summarized in Table 3 are obtained. Finally, the maps in Fig. 3 clearly show the convergence of the approximating sequence of functions $u_{L,M,N}(x,y,z)$ to the boundary values $h(x,y,z)$.

$N = 7$

$e_{L,M,N}$	$L = 1$	$L = 20$	$L = 40$
$M = 0$	74.812%	74.479%	74.455%
$M = 20$	108.604%	105.327%	105.156%
$M = 40$	27.579%	7.708%	4.822%

(a)

$M = 40$

$e_{L,M,N}$	$L = 1$	$L = 20$	$L = 40$
$N = 1$	29.618%	13.270%	11.830%
$N = 4$	27.664%	7.757%	4.841%
$N = 7$	27.578%	7.708%	4.822%

(b)

$L = 40$

$e_{L,M,N}$	$M = 0$	$M = 20$	$M = 40$
$N = 1$	51.820%	11.857%	11.830%
$N = 4$	74.206%	4.909%	4.841%
$N = 7$	74.455%	105.156%	4.822%

(c)

Table 2: Relative boundary error $e_{L,M,N}$ for different expansion orders of the Fourier-like solution of the Dirichlet problem for the Laplace equation (2.5) in a cylindrical domain $\mathcal{C}$, whose directrix is described by the polar equation (5.1) with parameters $\alpha = \beta = 3/4$, $m_1 = m_2 = 5$, $n_1 = n_2 = 7$, $n_3 = 2$.

$N = 11$

$e_{L,M,N}$	$L = 1$	$L = 20$	$L = 40$
$M = 0$	94.972%	87.623%	87.361%
$M = 20$	529.004%	526.539%	526.418%
$M = 40$	52.954%	14.204%	8.614%

(a)

$M = 40$

$e_{L,M,N}$	$L = 1$	$L = 20$	$L = 40$
$N = 1$	54.791%	19.993%	16.497%
$N = 6$	53.082%	14.674%	9.369%
$N = 11$	52.954%	14.204%	8.614%

(b)

$L = 40$

$e_{L,M,N}$	$M = 0$	$M = 20$	$M = 40$
$N = 1$	64.702%	16.592%	16.497%
$N = 6$	77.781%	9.535%	9.369%
$N = 11$	87.361%	526.418%	8.614%

(c)

Table 3: Relative boundary error $e_{L,M,N}$ for different expansion orders of the Fourier-like solution of the Dirichlet problem for the Laplace equation (2.5) in a cylindrical domain $\mathcal{C}$, whose directrix is described by the polar equation (5.1) with parameters $\alpha = \beta = 1/8$, $m_1 = 5$, $m_2 = 7$, $n_1 = n_2 = 5$, $n_3 = 17$.

5.4 Example 4

By assuming in (5.1) $\alpha = \beta = 1$, $m_1 = m_2 = 10$, $n_1 = n_2 = 1$, $n_3 = 7$, and $\theta \in [0, 4\pi]$, the domain $\mathcal{C}$ features the polygonal shape shown in Fig. 4. Let

	$e_{L,M,N}$	$L=1$	$L=20$	$L=40$
$N=11$	$M=0$	91.353%	91.353%	91.353%
	$M=20$	30.397%	13.381%	12.641%
	$M=40$	30.378%	12.429%	11.298%

(*a*)

	$e_{L,M,N}$	$L=1$	$L=20$	$L=40$
$M=40$	$N=1$	32.164%	16.315%	15.471%
	$N=6$	30.382%	12.438%	11.308%
	$N=11$	30.378%	12.429%	11.298%

(*b*)

	$e_{L,M,N}$	$M=0$	$M=20$	$M=40$
$L=40$	$N=1$	91.479%	16.477%	15.471%
	$N=6$	91.353%	12.651%	11.308%
	$N=11$	91.353%	12.641%	11.298%

(*c*)

Table 4: Relative boundary error $e_{L,M,N}$ for different expansion orders of the Fourier-like solution of the Dirichlet problem for the Laplace equation (2.5) in a cylindrical domain $\mathcal{C}$, whose directrix is described by the polar equation (5.1) with parameters $\alpha=\beta=1$, $m_1=m_2=10$, $n_1=n_2=1$, $n_3=7$.

$f_0(x,y) = \left(1-x^2-y^2\right)(\cos x \sin y - xy)$, $f_1(x,y) = e^{-3x^2-2y^2}\mathrm{Im}\left\{\sqrt{-x+iy}\right\}$, and $g(x,y,z) = \left(z-z^2\right)\left[\log\left(1+x^2+y^2+z^2\right)+\sin(8xyz)\right]$ be the functions describing the boundary values. Then, as regards the relative boundary error $e_{L,M,N}$, the numerical results summarized in Table 4 are obtained. Finally, the maps in Fig. 4 clearly show the convergence of the approximating sequence of functions $u_{L,M,N}(x,y,z)$ to the boundary values $h(x,y,z)$.

Remark 5. *We note that when the boundary values have wide oscillations, it is necessary to increase the number of terms in the relevant Fourier expansion, in order to obtain better results.*

Remark 6. *The L^2 norm of the difference between the exact solution and its approximate values is always vanishing in the interior of the considered domain, and generally small on the boundary. Point-wise convergence seems to be true on the whole boundary, with only exception of a set of measure zero, corresponding to singular points for the function or its derivative. In these points oscillations of the approximate solution, recalling the classical Gibbs phenomenon, usually appear.*

6 Conclusion

It seems that the use of stretched co-ordinate system, reducing every starlike domain to a circle, allows to use the classical Fourier methods to a very large class of domains, permitting to find solutions in a closed form, and to avoid some more cumbersome techniques such as the conformal mapping theorem, and the finite difference methods, since it is possible to use only quadrature rules and solution of linear systems.

An extension to three dimensional starlike domains, by using the spherical co-ordinate system, is presented in this volume.

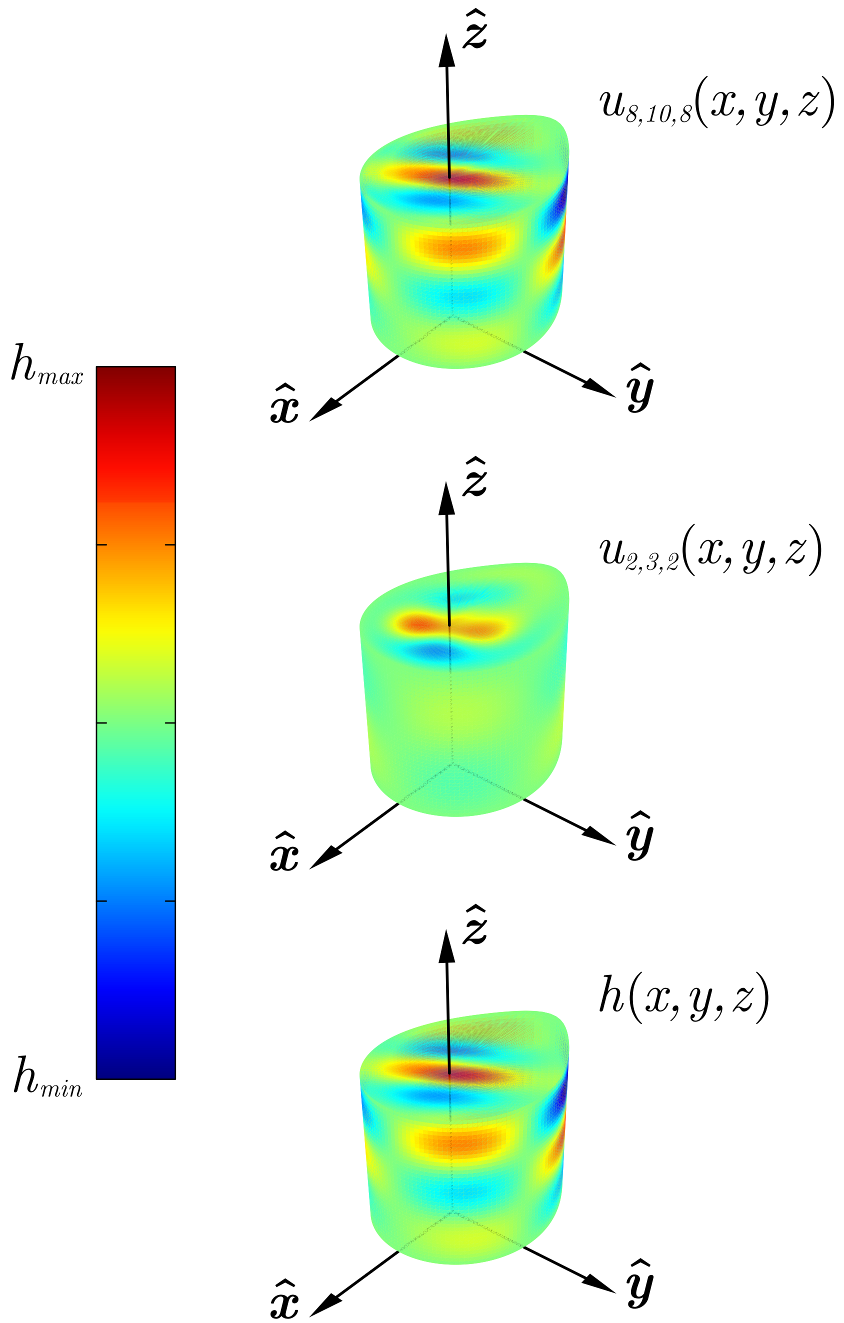

Figure 1: Boundary distribution of Fourier-type expansions $u_{L,M,N}(x,y,z)$ approximating the solution of the Dirichlet problem for the Laplace equation (2.5) in a cylindrical domain $\mathcal{C}$, whose directrix is described by the polar equation (5.1) with parameters $\alpha = 1/8$, $\beta = 1$, $m_1 = m_2 = 2$, $n_1 = 2$, $n_2 = n_3 = 6$.

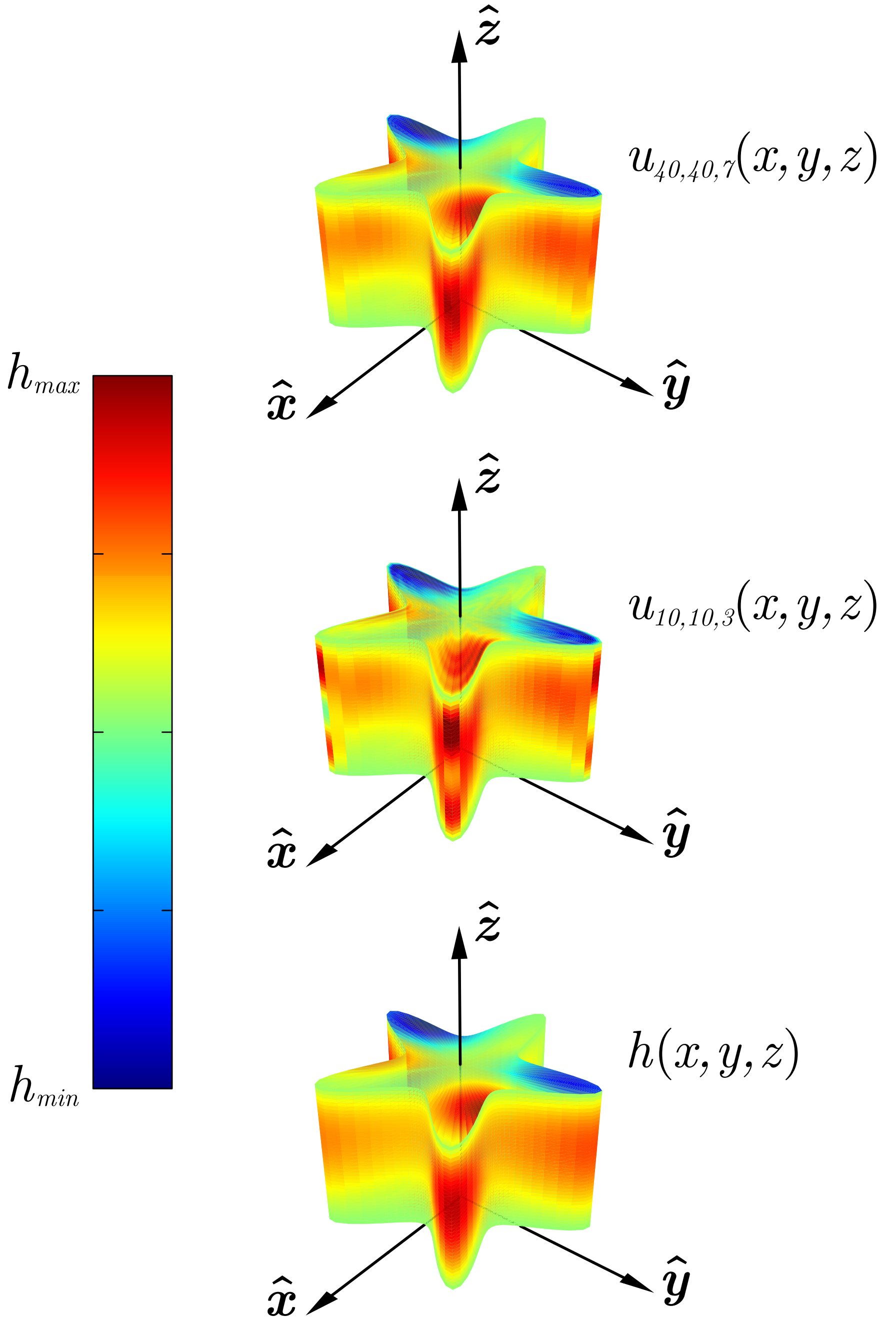

Figure 2: Boundary distribution of Fourier-type expansions $u_{L,M,N}\,(x,y,z)$ approximating the solution of the Dirichlet problem for the Laplace equation (2.5) in a cylindrical domain $\mathcal{C}$, whose directrix is described by the polar equation (5.1) with parameters $\alpha = \beta = 3/4$, $m_1 = m_2 = 5$, $n_1 = n_2 = 7$, $n_3 = 2$. Gibbs-like phenomena can be easily noticed at the quasi-cusped points of the domain.

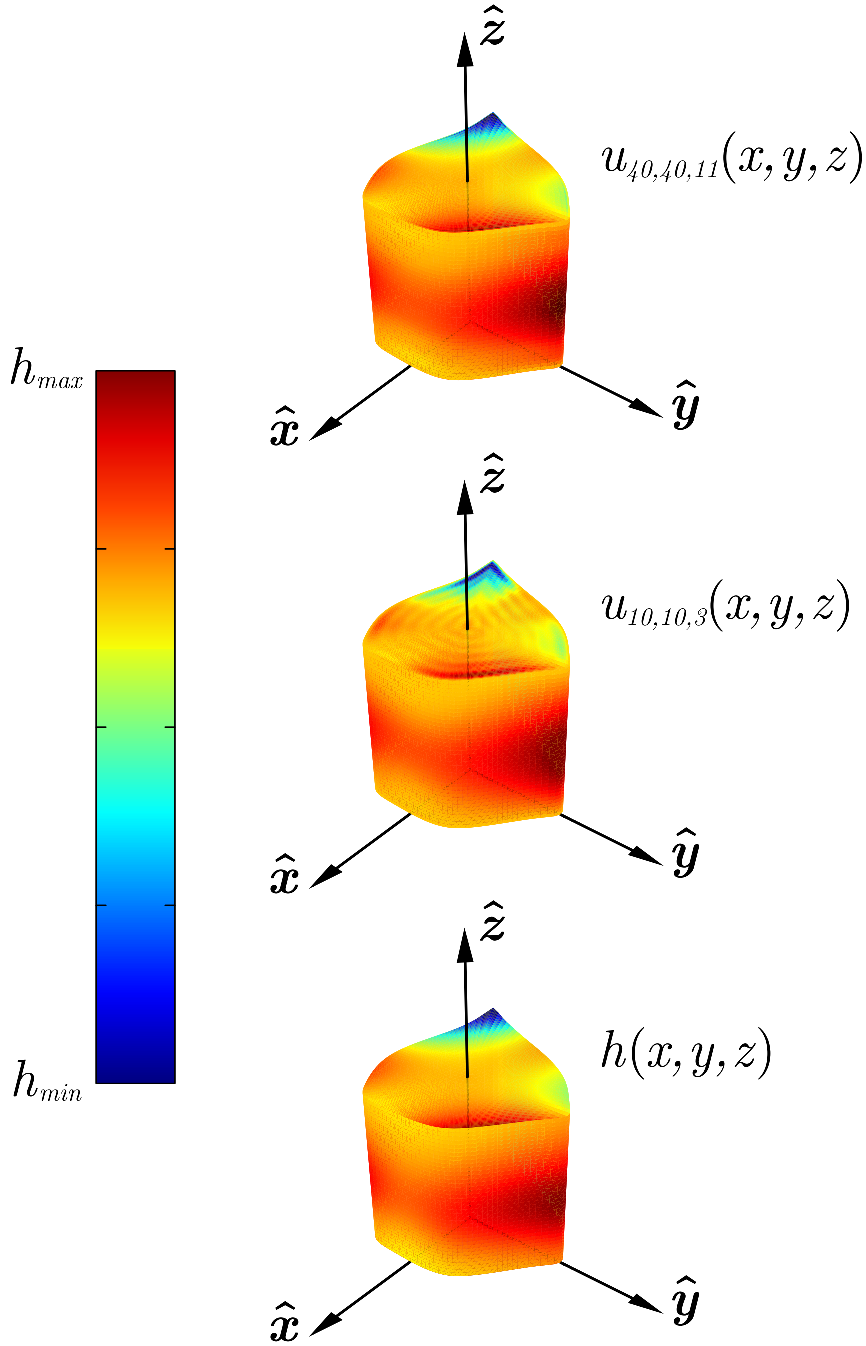

Figure 3: Boundary distribution of Fourier-type expansions $u_{L,M,N}\,(x,y,z)$ approximating the solution of the Dirichlet problem for the Laplace equation (2.5) in a cylindrical domain $\mathcal{C}$, whose directrix is described by the polar equation (5.1) with parameters $\alpha = \beta = 1/8$, $m_1 = 5$, $m_2 = 7$, $n_1 = n_2 = 5$, $n_3 = 17$.

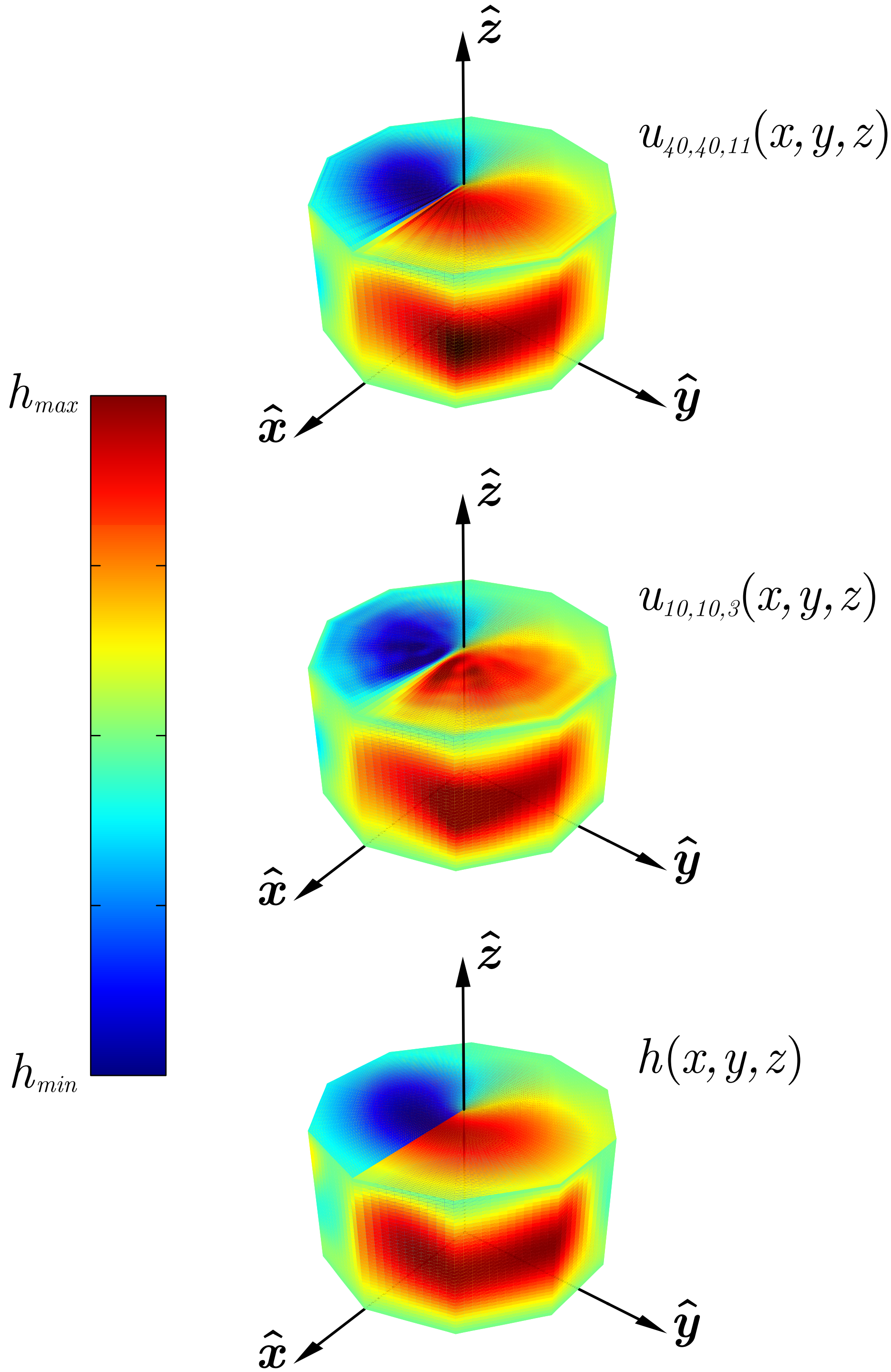

Figure 4: Boundary distribution of Fourier-type expansions $u_{L,M,N}(x,y,z)$ approximating the solution of the Dirichlet problem for the Laplace equation (2.5) in a cylindrical domain $\mathcal{C}$, whose directrix is described by the polar equation (5.1) with parameters $\alpha = \beta = 1$, $m_1 = m_2 = 10$, $n_1 = n_2 = 1$, $n_3 = 7$.

Acknowledgments - This research has been carried out under a grant by Italian PRIN/2006 Cap.7320.

References

[1] P. Natalini, P.E. Ricci, The Laplacian in stretched polar co-ordinates and Applications, *Proceedings ISAAC Conference on "Complex Analysis, Partial Differential Equations and Mechanics of Continua", dedicated to the Centenary of Ilia Vekua*, (to appear).

[2] P. Natalini, R. Patrizi, P.E. Ricci, The Dirichlet problem for the Laplace equation in a starlike domain of a Riemann surface, Numer. Algorithms, (to appear).

[3] L.C. Andrews, *Special functions of Mathematics for Engineers*, Oxford Univ. Press, Oxford - New York, 1998.

[4] G. Krall, *Meccanica Tecnica delle Vibrazioni*, Vol. II, Veschi, Roma, 1970.

[5] D. Medková, Solution of the dirichlet problem for the Laplace equation, *Appl. Math.*, **44**, (1999), 143–168.

[6] G.T. Golovin, M.M. Makarov, M.N. Sablin, D.V. Sukhachev, V.M. Yakovlev, Solution of the Dirichlet problem for the Laplace equation in irregular regions: comparison of different methods, *USSR Computational Mathematics and Mathematical Physics archive*, **27**, (1987), 40–50, Pergamon Press, Inc.

[7] B.N. Khoromskiĭ, Integro-difference method of solution of the Dirichlet problem for the Laplace equation. (Russian) *Zh. Vychisl. Mat. i Mat. Fiz.*, **24**, (1984), 53–64.

[8] A.P. Volkov, An effective method for solving the Dirichlet problem for the Laplace equation. (Russian) *Differentsial′nye Uravneniya* **19**, (1983), 1000–1007.

[9] A.P. Volkov, On the grid method for solving the Dirichlet problem for the Laplace equation in a cylinder with lateral surface of class $C^{1,1}$ Russian J. Num. Anal. Math. Model., **15** 6, (2000), 521–538.

[10] N.S. Bahvalov, A method for an approximate solution of Laplace's equation, (Russian) Dokl. Akad. Nauk SSSR (N.S.), **114** (1957), 455–458.

[11] D.M. Young, Iterative methods for solving partial difference equations of elliptic type, *Trans. Amer. Math. Soc.* **76**, (1954), 92–111.

[12] A.V. Bitsadze, A.A. Samarskii, On the Simplest Generalizations of Linear Elliptic Problems. (Russian), *Dokl. Akad. Nauk SSSR*, **185**, 1969, No. 4, 739–740.

[13] D. Gordeziani, N. Gordeziani, G. Avalishvili, On the Investigation and Resolution of Non-Local Boundary and Initial-Boundary Value Problems, *Reports of Enlarged Session of I. Vekua Inst. of Appl. Math.*, Tbilisi State Univ., **12**, 1997, No. 3.

[14] J. Gielis, A Generic geometric transformation that unifies a wide range of natural and Abstract Shapes, *Amer. J. Botany*, **90** , (2003), 333–338.

[15] L. Carleson, On convergence and growth of partial sums of Fourier series. *Acta Math.*, **116** (1966), 135–157.

[16] G.P. Tolstov, *Fourier series*, Transl. from Russian by R.A. Silverman, Dover Publ. Inc., New York, 1962.

[17] D. Caratelli, P.E. Ricci, The Dirichlet problem for the Laplace equation in a starlike domain, Proc. Intern. Conf. Scientific Computing (WORLDCOMP'08), Las Vegas, (to appear).

The Dirichlet problem for the Laplace equation in a starlike domain

by **Diego Caratelli** (*) and **Paolo E. Ricci** (†)

(*) *Delft University of Technology, IRCTR,*
Mekelweg, 4 – 2628 CD, Delft, the Netherlands
e-mail: d.caratelli@tudelft.nl

(†) *Università di Roma "La Sapienza", Dipartimento di Matematica,*
P.le A. Moro, 2 – 00185, Roma, Italia
e-mail: riccip@uniroma1.it

Abstract. We consider the Dirichlet problem for the Laplace equation in a starlike domain, i.e. a domain which is normal with respect to a suitable spherical co-ordinates system. Such a domain can be interpreted as a non-isotropically stretched unit sphere.

We write down the explicit solution in terms of a Fourier series whose coefficients are determined by solving an infinite system of linear equations depending on the boundary data.

Numerical experiments show that our method guarantees almost everywhere convergence, whenever the boundary data belong to L^2, in accordance with the results proved by L. Carleson.

AMS CLASSIFICATION: 35J05, 35J25.
KEY WORDS: Dirichlet problem. Laplace equation, starlike domain.

1 Introduction

Many applications of Mathematical Physics and Engineering are connected with the Laplacian.

- The wave equation $v_{tt} = a^2 \, \Delta v$
- The heat propagation $v_t = \kappa \, \Delta v$
- The Laplace equation $\Delta v = 0$
- The Helmholtz equation $\Delta v + k^2 v = 0$
- The Poisson equation $\Delta v = f$
- The Schrödinger equation $-\dfrac{h^2}{2m} \, \Delta \psi + V \psi = E \psi \,,$

however, the most part of boundary value problems (shortly BVP) relevant to the Laplacian are solved in explicit form only for domains with a very special shape, namely intervals, cylinders or domains with special (circular or spherical) symmetries [1].

The solution for more general domains is obtained by using the Riemann theorem on conformal mappings, and the relevant invariance of the Laplacian [2]. However, explicit conformal mappings are known only for particular domains. Of course, this method does not exist in the three-dimensional case, and the usual approach makes use of discretization.

Different techniques was also used for solving the general problem, both from a theoretical and computational point of view (see e.g. [3], representing solution by using boundary layer techniques; [4], comparing several numerical methods; [5], solving by iterative methods the corresponding boundary integral equation; [6], approximating the relevant Green function by the least squares method; [7], considering the system of linear equations arising from an unusual finite difference approximation; [8], solving linear systems relevant to elliptic partial differential equations by relaxation methods). However, none of the articles we have found in literature is connected with our approach, which makes use of simple tools, tracing back to the original Fourier method.

We consider in this article an extension of the classical theory to the case of a starlike domain, i.e. a domain $\mathcal{D}$, which is normal with respect to a suitable spherical co-ordinate system.

In Chapter 1, considering the two-dimensional case, we have shown how to write down explicitly the solution of the Dirichlet problem for the Laplace equation in terms of a Fourier series whose coefficients are determined by solving an infinite linear system, depending on the boundary data [9]. The integral operator which is naturally connected with this system is compact, and therefore, by using F. Riesz'theory [10], its solution can be approximated by solving a finite dimensional linear system, since the error term can be shown to be negligible, when the finite dimension increases.

In this article we consider further applications of the above mentioned method extending results to the case of three-dimensional domains. The boundary of the domains we have considered in all our applications are defined by generalizing the so called "superformula" due to J. Gielis [12].

The numerical examples, computed by using the Computer Algebra program Mathematica©, confirm, even in the above mentioned more general case the theoretical results of L. Carllson [13], since we have found a point-wise convergence in all regular points of the boundary, with possible oscillation usually occurring only in singular points.

2 The Laplacian in stretched spherical co-ordinates

We introduce in the three-dimensional space the ordinary spherical co-ordinate system:

$$x = r\,\cos\varphi\sin\vartheta\,, \quad y = r\sin\varphi\sin\vartheta\,, \quad z = r\cos\vartheta\,, \tag{2.1}$$

and the polar equation of $\partial\mathcal{D}$

$$r = R(\vartheta,\varphi) \qquad (0 \le \vartheta \le \pi\,; \quad 0 \le \varphi \le 2\pi)\ , \tag{2.2}$$

where $R(\vartheta,\varphi)$ is a piece-wise C^2 function in $[0,\pi]\times[0,2\pi]$. We suppose the domain $\mathcal{D}$ satisfies

$$0 < A \le r \le R(\vartheta,\varphi)\,,$$

and therefore $\min\limits_{(\vartheta,\varphi)\in[0,\pi]\times[0,2\pi]} R(\vartheta,\varphi) > 0.$

We introduce the stretched radius ρ such that

$$r = \rho\,R(\vartheta,\varphi)\,, \tag{2.3}$$

and the curvilinear (i.e. stretched) co-ordinates ρ, ϑ, φ , in the space x, y, z,

$$x = \rho\, R(\vartheta, \varphi)\, \cos\varphi \sin\vartheta\,,\ y = \rho\, R(\vartheta, \varphi)\, \sin\varphi \sin\vartheta\,,\ z = \rho\, R(\vartheta, \varphi)\, \cos\vartheta\,. \tag{2.4}$$

Therefore, $\mathcal{D}$ is obtained assuming $0 \le \vartheta \le \pi\,,\ 0 \le \varphi \le 2\pi\,,\ 0 \le \rho \le 1\,.$

Remark 7. – Note that, in the stretched co-ordinate system the original domain $\mathcal{D}$ is transformed into the unit sphere, so that in this system we can use for the transformed Laplace equation all the classical techniques, including separation of variables.

We consider a $C^2(\mathcal{D})$ function $v(x, y, z) = v(r\cos\varphi \sin\vartheta, r\sin\varphi\sin\vartheta, r\cos\vartheta) = u(r, \vartheta, \varphi)$ and the Laplace operator in spherical co-ordinates

$$\Delta u = \frac{1}{r^2}\frac{\partial}{\partial r}\left(r^2\frac{\partial u}{\partial r}\right) + \frac{1}{r^2\sin\vartheta}\frac{\partial}{\partial\vartheta}\left(\sin\vartheta\frac{\partial u}{\partial\vartheta}\right) + \frac{1}{r^2\sin^2\vartheta}\frac{\partial^2 u}{\partial\varphi^2}\,. \tag{2.5}$$

We start representing this operator in the new stretched co-ordinate system ρ, ϑ, φ. Setting

$$U(\rho, \vartheta, \varphi) = u\left(\rho R(\vartheta, \varphi), \vartheta, \varphi\right)\,, \tag{2.6}$$

we find (denoting for shortness $R := R(\vartheta, \varphi)$),

$$\frac{\partial u}{\partial r} = \frac{1}{R}\frac{\partial U}{\partial\rho}\,, \tag{2.7}$$

$$\frac{\partial^2 u}{\partial r^2} = \frac{1}{R^2}\frac{\partial^2 U}{\partial\rho^2}\,, \tag{2.8}$$

$$\frac{\partial u}{\partial\vartheta} = -\rho\frac{R_\vartheta}{R}\frac{\partial U}{\partial\rho} + \frac{\partial U}{\partial\vartheta}\,, \tag{2.9}$$

$$\frac{\partial^2 u}{\partial\vartheta^2} = \rho\,\frac{2R_\vartheta^2 - RR_{\vartheta\vartheta}}{R^2}\frac{\partial U}{\partial\rho} + \rho^2\frac{R_\vartheta^2}{R^2}\frac{\partial^2 U}{\partial\rho^2} - 2\rho\frac{R_\vartheta}{R}\frac{\partial^2 U}{\partial\rho\partial\vartheta} + \frac{\partial^2 U}{\partial\vartheta^2}\,. \tag{2.10}$$

$$\frac{\partial u}{\partial\varphi} = -\rho\frac{R_\varphi}{R}\frac{\partial U}{\partial\rho} + \frac{\partial U}{\partial\varphi}\,, \tag{2.11}$$

$$\frac{\partial^2 u}{\partial\varphi^2} = \rho\,\frac{2R_\varphi^2 - RR_{\varphi\varphi}}{R^2}\frac{\partial U}{\partial\rho} + \rho^2\frac{R_\varphi^2}{R^2}\frac{\partial^2 U}{\partial\rho^2} - 2\rho\frac{R_\varphi}{R}\frac{\partial^2 U}{\partial\rho\partial\varphi} + \frac{\partial^2 U}{\partial\varphi^2}\,. \tag{2.12}$$

Substituting we find our result, i.e.

$$\begin{aligned}
\Delta u &= \frac{\partial^2 u}{\partial r^2} + \frac{2}{r}\frac{\partial u}{\partial r} + \frac{1}{r^2}\frac{\partial^2 u}{\partial\vartheta^2} + \frac{\cot\vartheta}{r^2}\frac{\partial u}{\partial\vartheta} + \frac{1}{r^2\sin^2\vartheta}\frac{\partial^2 u}{\partial\varphi^2} \\
&= \frac{1}{R^2}\left[1 + \frac{R_\vartheta^2}{R^2} + \frac{R_\varphi^2}{R^2\sin^2\vartheta}\right]\frac{\partial^2 U}{\partial\rho^2} \\
&+ \frac{1}{\rho R^2}\left[2\left(1 + \frac{R_\vartheta^2}{R^2} + \frac{R_\varphi^2}{R^2\sin^2\vartheta}\right) - \frac{1}{R}\left(R_\vartheta\cot\vartheta + R_{\vartheta\vartheta} + \frac{R_{\varphi\varphi}}{\sin^2\vartheta}\right)\right]\frac{\partial U}{\partial\rho} \\
&- 2\frac{R_\vartheta}{\rho R^3}\frac{\partial^2 U}{\partial\rho\partial\vartheta} - 2\frac{R_\varphi}{\rho R^3\sin^2\vartheta}\frac{\partial^2 U}{\partial\rho\partial\varphi} \\
&+ \frac{1}{\rho^2 R^2}\frac{\partial^2 U}{\partial\vartheta^2} + \frac{\cot\vartheta}{\rho^2 R^2}\frac{\partial U}{\partial\vartheta} + \frac{1}{\rho^2 R^2\sin^2\vartheta}\frac{\partial^2 U}{\partial\varphi^2}\,.
\end{aligned} \tag{2.13}$$

For $\rho = r\,,\ R(\vartheta,\varphi) \equiv 1$, we recover the Laplacian in spherical co-ordinates.

3 An equivalent formulation

For further computations, it is easier to change the spherical equation of $\partial\mathcal{D}$ by setting

$$\Upsilon := \Upsilon\,(\vartheta,\varphi) := \frac{1}{R\,(\vartheta,\varphi)} \qquad (0 \le \vartheta \le \pi\,; \quad 0 \le \varphi \le 2\pi). \tag{3.1}$$

The unit sphere is recovered whenever $\Upsilon\,(\vartheta,\varphi) \equiv 1$.

Using this spherical equation, the corresponding stretched co-ordinates ρ, ϑ, φ, in the space x, y, z, are given by

$$x = \frac{\rho}{\Upsilon\,(\vartheta,\varphi)}\,\cos\varphi\sin\vartheta\,,\ y = \frac{\rho}{\Upsilon\,(\vartheta,\varphi)}\,\sin\varphi\sin\vartheta\,,\ z = \frac{\rho}{\Upsilon\,(\vartheta,\varphi)}\,\cos\vartheta\,, \tag{3.2}$$

and assuming again, for shortness:

$$U\,(\rho,\vartheta,\varphi) = u\left(\frac{\rho}{\Upsilon\,(\vartheta,\varphi)}, \vartheta, \varphi\right),$$

the Laplacian becomes:

$$\begin{aligned}\Delta u = \left(\Upsilon^2 + \Upsilon_\vartheta^2 + \frac{\Upsilon_\varphi^2}{\sin^2\vartheta}\right)\frac{\partial^2 U}{\partial\rho^2} + \frac{\Upsilon}{\rho}\left(2\Upsilon + \Upsilon_\vartheta\cot\vartheta + \Upsilon_{\vartheta\vartheta} + \frac{\Upsilon_{\varphi\varphi}}{\sin^2\vartheta}\right)\frac{\partial U}{\partial\rho} \\ + \frac{2\Upsilon\Upsilon_\vartheta}{\rho}\,\frac{\partial^2 U}{\partial\rho\partial\vartheta} + \frac{2\Upsilon\Upsilon_\varphi}{\rho\sin^2\vartheta}\,\frac{\partial^2 U}{\partial\rho\partial\varphi} + \frac{\Upsilon^2}{\rho^2}\,\frac{\partial^2 U}{\partial\vartheta^2} \\ + \frac{\Upsilon^2\cot\vartheta}{\rho^2}\,\frac{\partial U}{\partial\vartheta} + \frac{\Upsilon^2}{\rho^2\sin^2\vartheta}\,\frac{\partial^2 U}{\partial\varphi^2}\,.\end{aligned} \tag{3.3}$$

For $\rho = r\,,\ \Upsilon\,(\vartheta,\varphi) \equiv 1$, we find again the Laplacian in spherical co-ordinates.

4 Applications to the Dirichlet problem

Consider the Dirichlet problem for the Laplace equation

$$\begin{cases} \Delta u(r,\vartheta,\varphi) = 0\,, & r < R(\vartheta,\varphi) \quad (0 \le \vartheta \le \pi\,,\ 0 \le \varphi < 2\pi)\,, \\ u(r,\vartheta,\varphi) = f(\vartheta,\varphi)\,, & r = R(\vartheta,\varphi) \quad (0 \le \vartheta \le \pi\,,\ 0 \le \varphi < 2\pi)\,. \end{cases} \tag{4.1}$$

We prove the following result

Theorem 4.1. *Let*

$$f(\vartheta,\varphi)=\sum_{n=0}^{+\infty}\sum_{m=0}^{n}P_n^m(\cos\vartheta)\left(\alpha_{n,m}\cos m\varphi+\beta_{n,m}\sin m\varphi\right)\,, \tag{4.2}$$

where

$$\left\{\begin{array}{c}\alpha_{n,m}\\ \beta_{n,m}\end{array}\right\}=\epsilon_m\frac{2n+1}{4\pi}\,\frac{(n-m)!}{(n+m)!}\int_0^{2\pi}\!\!\int_0^{\pi}f(\vartheta,\varphi)P_n^m(\cos\vartheta)\left\{\begin{array}{c}\cos m\varphi\\ \sin m\varphi\end{array}\right\}\sin\vartheta d\vartheta\,d\varphi\,, \tag{4.3}$$

$\epsilon_m=\left\{\begin{array}{ll}1\,, & m=0\\ 2\,, & m\neq 0\end{array}\right.$ *, and P_n^m are the associated Legendre functions of the first kind* (see [1]).

Then, the solution of the interior Dirichlet problem *can be represented as*

$$u(r,\vartheta,\varphi)=\sum_{n=0}^{+\infty}\sum_{m=0}^{n}r^nP_n^m(\cos\vartheta)\left(A_{n,m}\cos m\varphi+B_{n,m}\sin m\varphi\right)\,, \tag{4.4}$$

where the coefficients $A_{n,m},B_{n,m}$ *can be found by solving the infinite linear system*

$$\sum_{n=0}^{+\infty}\sum_{m=0}^{n}\left[\begin{array}{cc}X^{+}_{n,m,h,k} & Y^{+}_{n,m,h,k}\\ X^{-}_{n,m,h,k} & Y^{-}_{n,m,h,k}\end{array}\right]\cdot\left[\begin{array}{c}A_{n,m}\\ B_{n,m}\end{array}\right]=\left[\begin{array}{c}\alpha_{h,k}\\ \beta_{h,k}\end{array}\right]\,,$$

$$(h\in\mathbf{N_0}\,,\ k=0,1,\ldots,h)\,, \tag{4.5}$$

where

$$X^{\pm}_{n,m,h,k}\;=\;\epsilon_k\frac{2h+1}{4\pi}\,\frac{(h-k)!}{(h+k)!}\int_0^{2\pi}\!\!\int_0^{\pi}\left[R(\vartheta,\varphi)\right]^n P_n^m(\cos\vartheta)P_h^k(\cos\vartheta)\cos m\varphi\left\{\begin{array}{c}\cos k\varphi\\ \sin k\varphi\end{array}\right\}\cdot$$
$$\cdot\sin\vartheta d\vartheta\,d\varphi\,,$$

$$Y^{\pm}_{n,m,h,k}\;=\;\epsilon_k\frac{2h+1}{4\pi}\,\frac{(h-k)!}{(h+k)!}\int_0^{2\pi}\!\!\int_0^{\pi}\left[R(\vartheta,\varphi)\right]^n P_n^m(\cos\vartheta)P_h^k(\cos\vartheta)\sin m\varphi\left\{\begin{array}{c}\cos k\varphi\\ \sin k\varphi\end{array}\right\}\cdot$$
$$\cdot\sin\vartheta d\vartheta\,d\varphi\,.$$

Proof. Recalling Remark 1, elementary solutions of the problem (4.1) can be searched in the form

$$u(r,\vartheta,\varphi)=U\left(\frac{\rho}{R(\vartheta,\varphi)}\,,\vartheta,\varphi\right)=P(r)\Theta(\vartheta)\Phi(\varphi)\,. \tag{4.6}$$

Substituting into the Laplace equation we find that the functions P,Θ,Φ must satisfy the ordinary differential equations

$$\left\{\begin{array}{l}r^2\,\dfrac{d^2P}{dr^2}+2r\,\dfrac{dP}{dr}-\lambda^2P=0\,,\\[2ex] \dfrac{1}{\sin\vartheta}\,\dfrac{d}{d\vartheta}\left(\sin\vartheta\,\dfrac{d\Theta}{d\vartheta}\right)+\left(\lambda^2-\dfrac{\mu^2}{\sin^2\vartheta}\right)\Theta=0\,,\\[2ex] \dfrac{d^2\Phi}{d\varphi^2}+\mu^2\Phi=0\,,\end{array}\right. \tag{4.7}$$

and therefore, by using very classical results, we find

$$\mu = m \in \mathbf{Z}\,,$$

$$\lambda^2 = n(n+1)\,, \qquad n \in \mathbf{N_0}$$

$$\Phi(\varphi) = a_m \cos m\varphi + b_m \sin m\varphi \qquad (a_m\,, b_m \text{ arbitrary constants})\,,$$

and for the interior problem:

$$P(r) = c_m r^n\,, \quad (c_m \text{ arbitrary constant})$$

$$\Theta(\vartheta) = d_{n,m} P_n^m(\cos\vartheta)\,, \quad (d_{n,m} \text{ arbitrary constant})\,,$$

where

$$P_n^m(\eta) = (-1)^m(1-\eta^2)^{m/2}\frac{d^m P_n(\eta)}{d\eta^m} = (-1)^m\,\frac{(1-\eta^2)^{m/2}}{2^n\,n!}\,\frac{d^{n+m}(\eta^2-1)^n}{d\eta^{n+m}}\;.$$

Therefore a general solution of the Laplace equation can be written in the form

$$u(r,\vartheta,\varphi) = \sum_{n=0}^{+\infty}\sum_{m=0}^{n} r^n P_n^m(\cos\vartheta)\,(A_{n,m}\cos m\varphi + B_{n,m}\sin m\varphi)\;. \tag{4.8}$$

Imposing the boundary condition

$$\begin{aligned} f(\vartheta,\varphi) &= U(1,\vartheta,\varphi) = u\,[R(\vartheta,\varphi),\vartheta,\varphi] \\ &= \sum_{n=0}^{+\infty}\sum_{m=0}^{n} [R(\vartheta,\varphi)]^n\,P_n^m(\cos\vartheta)\,(A_{n,m}\cos m\varphi + B_{n,m}\sin m\varphi)\;, \end{aligned} \tag{4.9}$$

we find for the unknown constants $A_{n,m}, B_{n,m}$ in the system (4.5). ■

Remark 8. – Note that, assuming the unessential condition $R(\vartheta,\varphi) \le M < 1$, $\forall(\vartheta,\varphi) \in [0,\pi]\times[0,2\pi]$, the system (4.5) can be solved in an approximate way by considering the corresponding finite system where $n = 0,1,\dots,N$, and $h = 0,1,\dots,N$, $k = 0,1,\dots,h$, and the solution is convergent when $N \to +\infty$.

Remark 9. – Note that the above considerations hold whenever the function $R(\vartheta,\varphi)$ is a piecewise continuous function, and if the boundary data are given by square integrable functions, not necessarily continuous, so that the relevant coefficients $\alpha_{h,k}, \beta_{h,k}$ in equation (4.3) are finite.

In a similar way the *exterior problem* could be treated, assuming the usual condition at infinity:

$$\lim_{\rho\to+\infty} u(\rho,\vartheta,\varphi) = 0\,,$$

uniformly with respect to ϑ and φ.

5 Numerical examples

In the following examples we assume for the boundary $\partial\mathcal{D}$ a general spherical equation of the type

$$R(\vartheta,\varphi) = c\left[\left|\frac{\sin\frac{p\vartheta}{2}\cos\frac{q\varphi}{4}}{\gamma_1}\right|^{\nu_1} + \left|\frac{\sin\frac{p\vartheta}{2}\sin\frac{q\varphi}{4}}{\gamma_2}\right|^{\nu_2} + \left|\frac{\cos\frac{p\vartheta}{2}}{\gamma_3}\right|^{\nu_3}\right]^{-1/\nu_0}, \tag{5.1}$$

($p, q, \gamma_1, \gamma_2, \gamma_3, \nu_0, \nu_1, \nu_2, \nu_3$ integral numbers), extending to the three-dimensional case the curves introduced by J. Gielis [12]. Moreover, let $F(x, y, z)$ denote the function representing boundary values. Under such assumptions, the following expression results

$$f(\vartheta,\varphi) = F\left(R(\vartheta,\varphi)\cos\varphi\sin\vartheta, R(\vartheta,\varphi)\sin\varphi\sin\vartheta, R(\vartheta,\varphi)\cos\vartheta\right). \tag{5.2}$$

In numerical experiments, computed by using Mathematica©, we assume different values of the nine parameters $p, q, \gamma_1, \gamma_2, \gamma_3, \nu_0, \nu_1, \nu_2, \nu_3$, obtaining very different shapes for the considered domain, including ellipsoids, Lamé-type domains (also called *Superellipsoids*), ovaloids, (p, q)-fold symmetric figures, and so on. We introduced furthermore an extra parameter c, in order to ensure the convergence condition $\max_{(\vartheta,\varphi)\in[0,\pi]\times[0,2\pi]} R(\vartheta,\varphi) \leq M < 1$. We emphasize that almost all three-dimensional normal-polar domains are described (or at least approximated in a close way) by the above mentioned surfaces.

In particular, to assess the performances of the proposed algorithm in terms of numerical accuracy and convergence rate, the relative boundary error has been evaluated as follows

$$e_N = \frac{\|U_N(1,\vartheta,\varphi) - f(\vartheta,\varphi)\|}{\|f(\vartheta,\varphi)\|}, \tag{5.3}$$

where $\|\cdot\|$ denotes the usual $L^2(\partial\mathcal{D})$ norm, and

$$U_N(\rho,\vartheta,\varphi) = \sum_{n=0}^{N}\sum_{m=0}^{n}\left[\rho R(\vartheta,\varphi)\right]^n P_n^m(\cos\vartheta)\left(A_{n,m}\cos m\varphi + B_{n,m}\sin m\varphi\right), \tag{5.4}$$

is the $N-th$ partial sum of the approximating spherical harmonics series (4.8).

5.1 Example 1

By assuming in (5.1) $\gamma_1 = 5$, $\gamma_2 = \gamma_3 = 4$, $m = 1$, $n = 2$, $\nu_0 = \nu_1 = \nu_2 = 6$, $\nu_3 = 2$, the domain $\mathcal{D}$ features the shape depicted in Fig. 1.

Let $F(x, y, z) = \sinh\left(\frac{x+y}{4}\right) + \log\left(1 + x^2 + y^2 + z^2\right)$ be the function representing boundary values. Then, the relative boundary error e_N as function of the number N of terms in the relevant expansion (5.4) exhibits the behavior shown in Fig. 2.

Finally, the maps in Fig. 3 clearly show the convergence rate of the approximating sequence of functions $U_N(1,\vartheta,\varphi)$ to the boundary values $f(\vartheta,\varphi)$.

5.2 Example 2

By assuming in (5.1) $\gamma_1 = \gamma_2 = \gamma_3 = 1$, $m = 2$, $n = 4$, $\nu_0 = \nu_1 = \nu_2 = \nu_3 = 1$, the domain $\mathcal{D}$ features the shape depicted in Fig. 4.

Let $F(x, y, z) = x^2y^2 - 5x^2z^2 - 10y^2z^2 + \sinh(x + y)$ be the function representing boundary values. Then, the relative boundary error e_N as function of the number N of terms in the relevant expansion (5.4) exhibits the behavior shown in Fig. 5.

Finally, the maps in Fig. 6 clearly show the convergence rate of the approximating sequence of functions $U_N(1,\vartheta,\varphi)$ to the boundary values $f(\vartheta,\varphi)$.

5.3 Example 3

By assuming in (5.1) $\gamma_1 = \gamma_2 = 1$, $\gamma_3 = 1/2$, $m = 2$, $n = 5$, $\nu_0 = \nu_3 = 2$, $\nu_1 = \nu_2 = 7$, the domain $\mathcal{D}$ features the shape depicted in Fig. 7.

Let $F(x, y, z) = x + y + z + \sin(xz) + \cos(yz)$ be the function representing boundary values. Then, the relative boundary error e_N as function of the number N of terms in the relevant expansion (5.4) exhibits the behavior shown in Fig. 8.

Finally, the maps in Fig. 9 clearly show the convergence rate of the approximating sequence of functions $U_N(1, \vartheta, \varphi)$ to the boundary values $f(\vartheta, \varphi)$.

Remark 10. We note that when the boundary values have wide oscillations, it is necessary to increase the number N of terms in the relevant spherical harmonics expansion, in order to obtain better results.

Remark 11. The L^2 norm of the difference between the exact solution and its approximate value is always vanishing in the interior of the considered domain, and in general small on the boundary. Point-wise convergence seems to be verified on the whole boundary, with only exception of a set of measure zero, corresponding to cusped or quasi-cusped points. In this points oscillations of the approximate solution, recalling the classical Gibbs phenomenon, usually appear.

6 Conclusion

The use of the normal spherical co-ordinates allow us to find close formulas for a wide set of classical problems, avoiding the use of mesh-based numerical techniques, such as the *Finite Element Method* (*FEM*) [14].

The application of the proposed method to the solution of the classical problems of a vibrating membrane and heat equation, relevant to normal-spherical shaped domains is in progress.

References

[1] L.C. Andrews, *Special Functions of Mathematics for Engineers*, Oxford Univ. Press, Oxford - New York, 1998.

[2] G. Krall, *Meccanica Tecnica delle Vibrazioni*, Vol. II, Veschi, Roma, 1970.

[3] D. Medková, Solution of the Dirichlet problem for the Laplace equation, *Appl. Math.*, **44**, (1999), 143–168.

[4] G.T. Golovin, M.M. Makarov, M.N. Sablin, D.V. Sukhachev, V.M. Yakovlev, Solution of the Dirichlet problem for the Laplace equation in irregular regions: comparison of different methods, *USSR Computational Mathematics and Mathematical Physics archive*, **27**, (1987), 40–50, Pergamon Press, Inc.

[5] B.N. Khoromskiĭ, Integro-difference method of solution of the Dirichlet problem for the Laplace equation. (Russian) *Zh. Vychisl. Mat. i Mat. Fiz.*, **24**, (1984), 53–64.

[6] A.P. Volkov, An effective method for solving the Dirichlet problem for the Laplace equation. (Russian) *Differentsial′nye Uravneniya* **19**, (1983), 1000–1007.

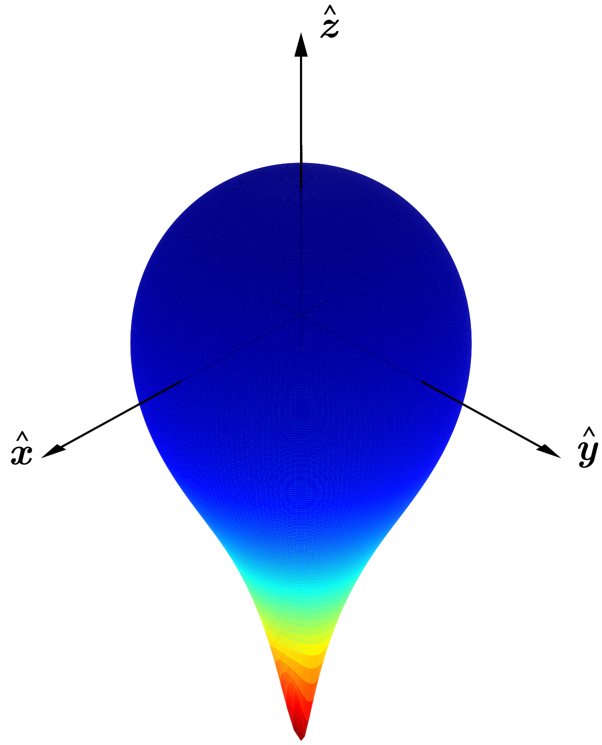

Figure 1: *Three-dimensional view of the domain* $\mathcal{D}$ *obtained by assuming in* (5.1) $\gamma_1 = 5, \gamma_2 = \gamma_3 = 4, m = 1, n = 2, \nu_0 = \nu_1 = \nu_2 = 6, \nu_3 = 2$. *The parameter* c *has been set in order to ensure the condition* $\max\limits_{(\vartheta,\varphi)\in[0,\pi]\times[0,2\pi]} R(\vartheta, \varphi) = 1$.

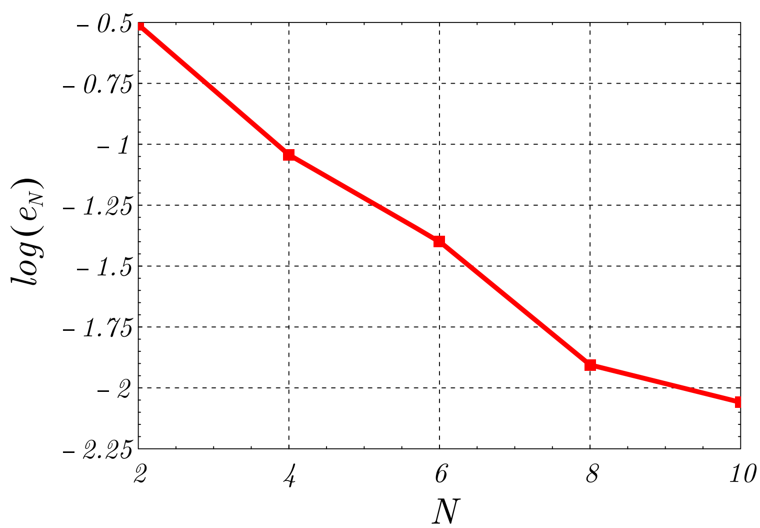

Figure 2: *Relative boundary error* e_N *as function of the number* N *of terms in the expansion* (5.4). *The relevant domain* $\mathcal{D}$ *is described by the spherical equation* (5.1) *with* $\gamma_1 = 5, \gamma_2 = \gamma_3 = 4, m = 1, n = 2, \nu_0 = \nu_1 = \nu_2 = 6, \nu_3 = 2$.

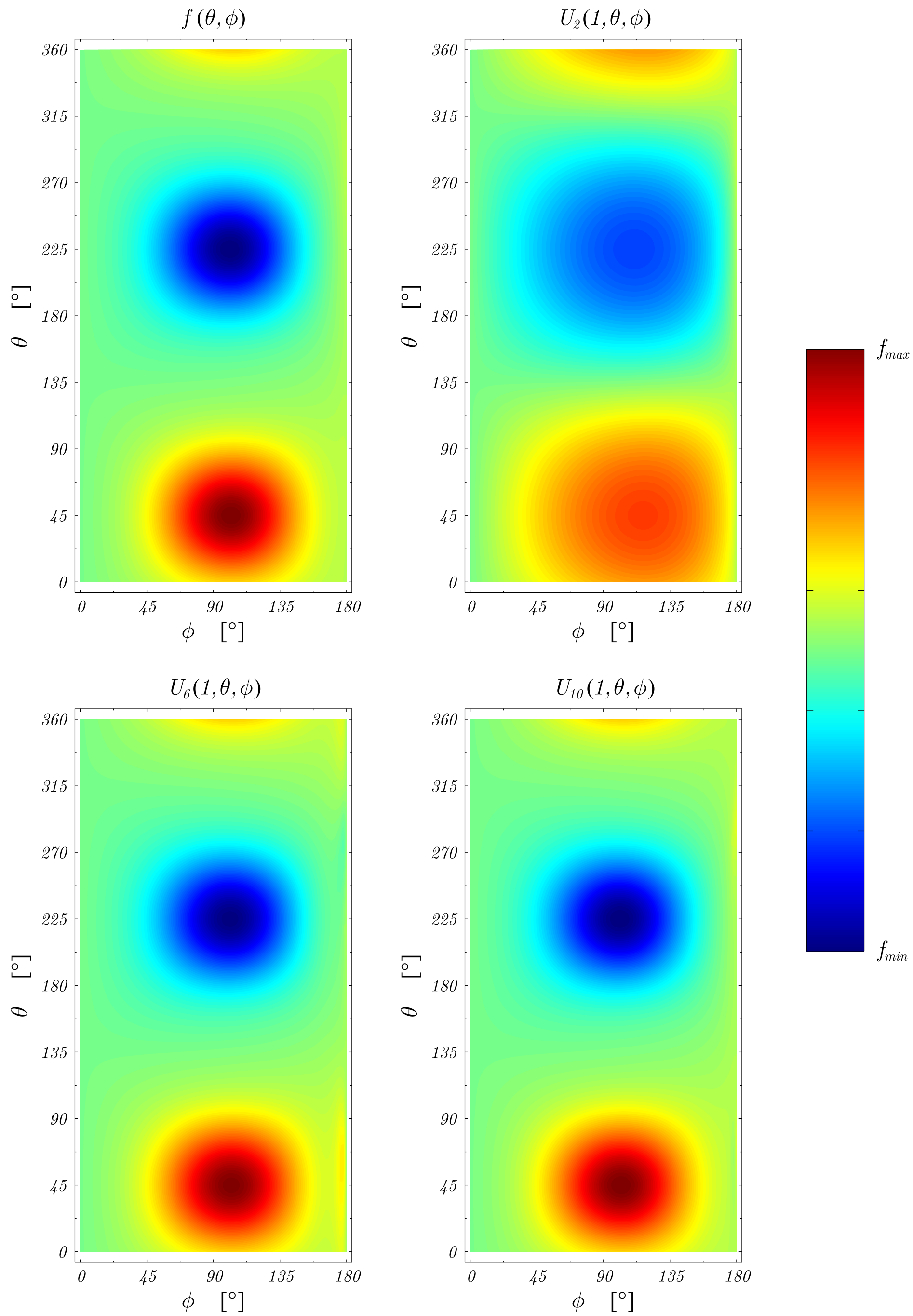

Figure 3: *Angular behavior of the* $N-th$ *partial sum of the approximating spherical harmonics series* $U_N(1,\vartheta,\varphi)$ *for different values of the expansion order* N. *A Gibbs-like phenomenon can be observed at the cusped point* $\vartheta = 180°$. *The relevant domain* $\mathcal{D}$ *is described by the spherical equation* (5.1) *with* $\gamma_1 = 5$, $\gamma_2 = \gamma_3 = 4$, $m = 1$, $n = 2$, $\nu_0 = \nu_1 = \nu_2 = 6$, $\nu_3 = 2$.

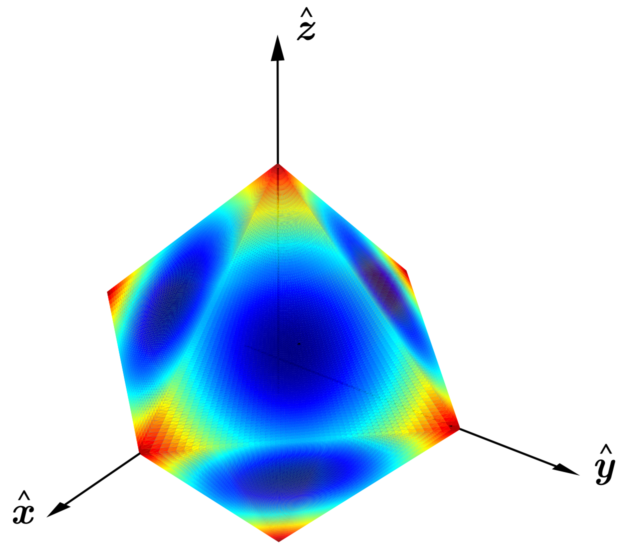

Figure 4: *Three-dimensional view of the domain* $\mathcal{D}$ *obtained by assuming in* (5.1) $\gamma_1 = \gamma_2 = \gamma_3 = 1$, $m = 2$, $n = 4$, $\nu_0 = \nu_1 = \nu_2 = \nu_3 = 1$. *The parameter* c *has been set in order to ensure the condition* $\max\limits_{(\vartheta,\varphi)\in[0,\pi]\times[0,2\pi]} R(\vartheta, \varphi) = 1$.

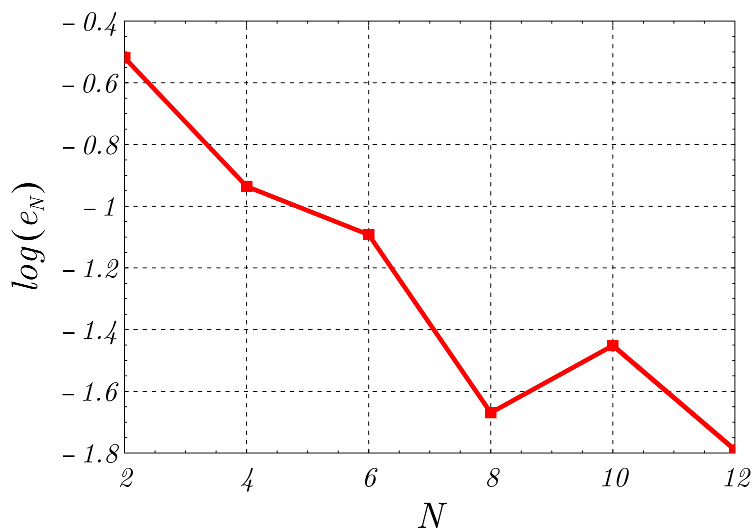

Figure 5: *Relative boundary error* e_N *as function of the number* N *of terms in the expansion* (5.4). *The relevant domain* $\mathcal{D}$ *is described by the spherical equation* (5.1) *with* $\gamma_1 = \gamma_2 = \gamma_3 = 1$, $m = 2$, $n = 4$, $\nu_0 = \nu_1 = \nu_2 = \nu_3 = 1$.

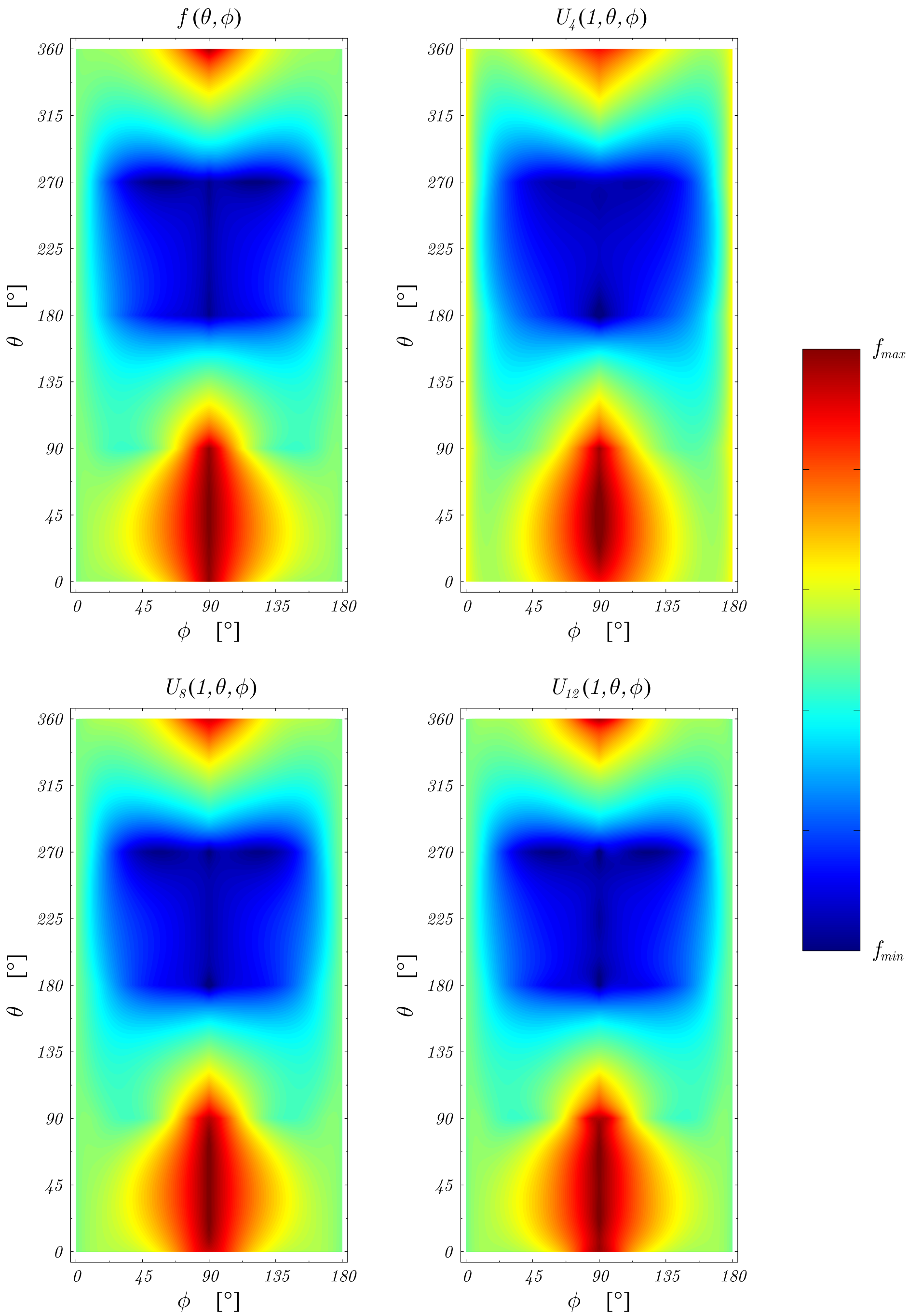

Figure 6: *Angular behavior of the* $N-th$ *partial sum of the approximating spherical harmonics series* $U_N(1,\vartheta,\varphi)$ *for different values of the expansion order* N*. Gibbs-like phenomena can be observed along the edges* $\vartheta = 90°$ *and* $\varphi = 0°, 90°, 180°, 270°$*. The relevant domain* $\mathcal{D}$ *is described by the spherical equation* (5.1) *with* $\gamma_1 = \gamma_2 = \gamma_3 = 1$, $m = 2$, $n = 4$, $\nu_0 = \nu_1 = \nu_2 = \nu_3 = 1$.

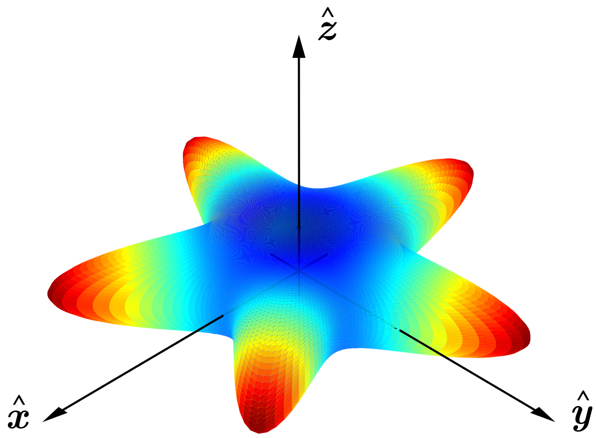

Figure 7: *Three-dimensional view of the domain* $\mathcal{D}$ *obtained by assuming in* (5.1) $\gamma_1 = \gamma_2 = 1$, $\gamma_3 = 1/2$, $m = 2$, $n = 5$, $\nu_0 = \nu_3 = 2$, $\nu_1 = \nu_2 = 7$. *The parameter* c *has been set in order to ensure the condition* $\max\limits_{(\vartheta,\varphi)\in[0,\pi]\times[0,2\pi]} R(\vartheta,\varphi) = 1$.

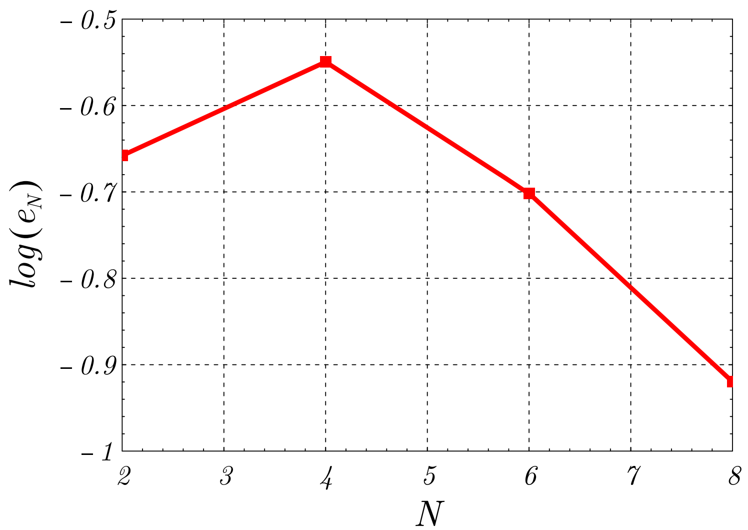

Figure 8: *Relative boundary error* e_N *as function of the number* N *of terms in the expansion* (5.4). *The relevant domain* $\mathcal{D}$ *is described by the spherical equation* (5.1) *with* $\gamma_1 = \gamma_2 = 1$, $\gamma_3 = 1/2$, $m = 2$, $n = 5$, $\nu_0 = \nu_3 = 2$, $\nu_1 = \nu_2 = 7$.

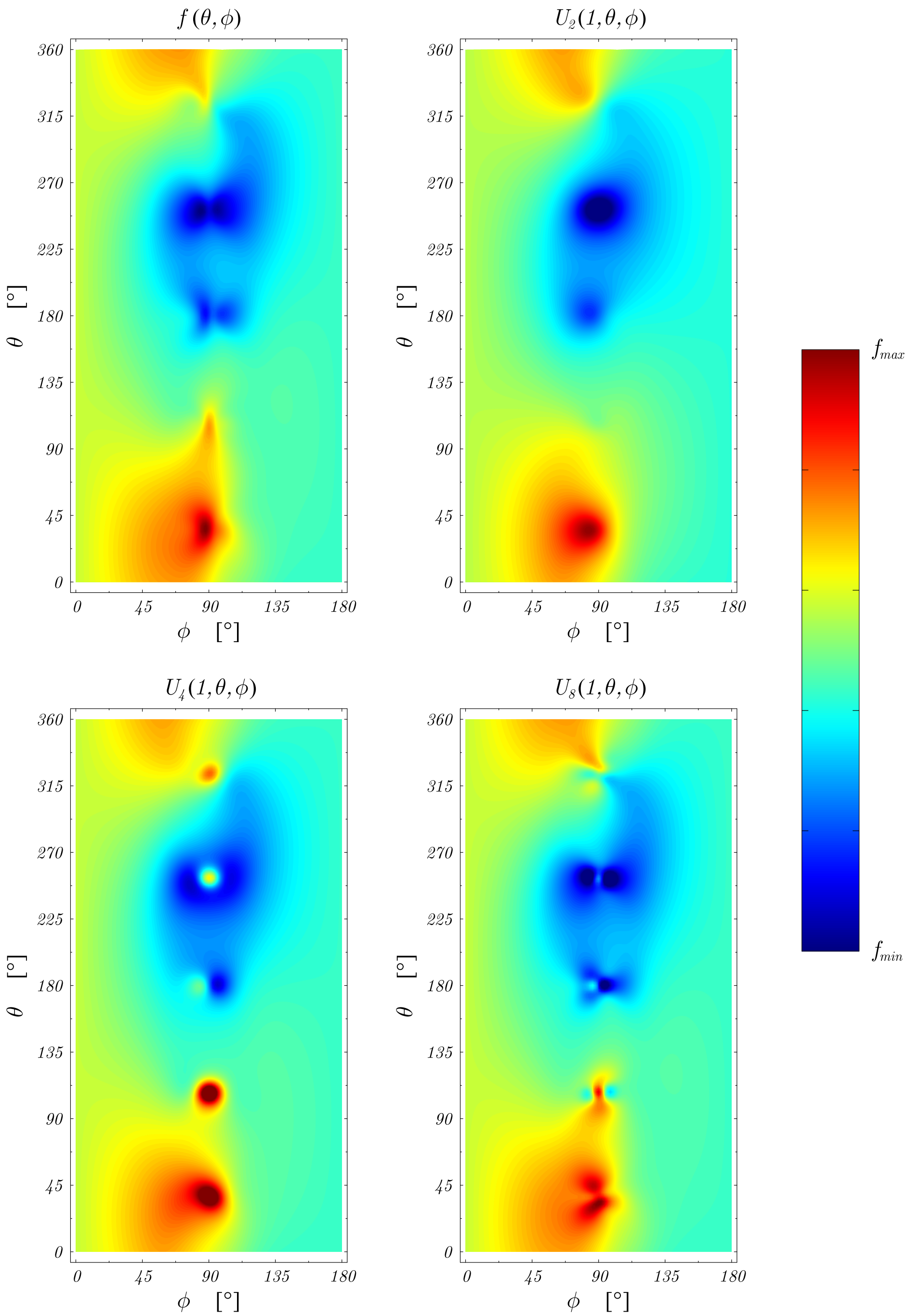

Figure 9: *Angular behavior of the* $N - th$ *partial sum of the approximating spherical harmonics series* $U_N(1, \vartheta, \varphi)$ *for different values of the expansion order* N. *Gibbs-like phenomena can be clearly observed at the quasi-cusped points of the relevant domain* $\mathcal{D}$, *which is described by the spherical equation* (5.1) *with* $\gamma_1 = \gamma_2 = 1$, $\gamma_3 = 1/2$, $m = 2$, $n = 5$, $\nu_0 = \nu_3 = 2$, $\nu_1 = \nu_2 = 7$.

[7] N.S. Bahvalov, A method for an approximate solution of Laplace's equation, (Russian) Dokl. Akad. Nauk SSSR (N.S.), **114** (1957), 455–458.

[8] D.M. Young, Iterative methods for solving partial difference equations of elliptic type, *Trans. Amer. Math. Soc.* **76**, (1954), 92–111.

[9] P. Natalini, P.E. Ricci, The Laplacian in stretched polar co-ordinates and Applications, *Proceedings ISAAC Conference on "Complex Analysis, Partial Differential Equations and Mechanics of Continua", dedicated to the Centenary of Ilia Vekua* (to appear).

[10] F. Riesz, *Les systèmes d'équations linéaires à une infinité d'inconnues*, Gauthier Villars, Paris, 1952.

[11] P. Natalini, R. Patrizi, P.E. Ricci, The Dirichlet problem for the Laplace equation in a starlike domain of a Riemann surface, Numer. Algorithms (to appear).

[12] J. Gielis, A Generic Geometric transformation that unifies a wide range of natural and Abstract Shapes, *Amer. J. Botany*, **90**, (2003), 333–338.

[13] L. Carleson, On convergence and growth of partial sums of Fourier series. *Acta Math.*, **116** (1966), 135–157.

[14] A. Bondeson, T. Rylander, P. Ingelstrom, *Computational Electromagnetics*, Springer Science, Texts in Applied Mathematics, New York, 2005.

The Dirichlet problem for the Helmholtz equation in a starlike domain

by **Diego Caratelli** [(⋆)] and **Paolo E. Ricci** [(†)]

[(⋆)] *Delft University of Technology, IRCTR*
Mekelweg 4, 2628 CD, Delft, the Netherlands

[(†)] *Università di Roma "La Sapienza", Dipartimento di Matematica*
P.le A. Moro, 2, 00185, Roma, Italia

Abstract. We consider the interior and exterior Dirichlet problem for the Helmholtz equation in a bounded starlike domain. We show how to construct the solution by using the Fourier series method. We derive some numerical results defining the boundary of the domain by means of the so called "superformula" introduced by J. Gielis. By using a computer algebra system we derive approximations satisfying properties similar to the classical ones. Our findings are in agreement with the theoretical results on Fourier series due to L. Carleson.

AMS CLASSIFICATION: 35J05, 35J25.

KEY WORDS: Dirichlet problem, Helmholtz equation, starlike domain, Fourier series.

1 Introduction

In recent articles [1], [2], [3], [4], the classical Fourier method [5], [6] for solving the Dirichlet problem for the Laplace equation in domains with very special (circular or spherical) symmetries was extended in order to solve the same problem in a starlike domain, i.e. a domain $\mathcal{D}$, which is normal with respect to a suitable spherical co-ordinate system. Note that $\mathcal{D}$ can be considered as a stretched unit sphere, centered at the origin.

We show in this article that similar results can be achieved even for the Helmholtz equation.

The boundary of domains we have considered in our last Section are defined by using the so called "superformula" due to J. Gielis [7].

Several numerical examples, computed by using the Computer Algebra system Mathematica©, confirm, even in the considered case, the theoretical results by L. Carleson [8], since we have found a point-wise convergence in all regular points of the boundary, with possible oscillation usually occurring only in singular points (for the function or its derivative).

2 The Laplacian in stretched spherical co-ordinates

We introduce in the three-dimensional space the ordinary spherical co-ordinate system:

$$x = r\,\cos\varphi\sin\vartheta\,, \quad y = r\sin\varphi\sin\vartheta\,, \quad z = r\cos\vartheta\,, \tag{2.1}$$

and the polar equation of $\partial\mathcal{D}$

$$r = R(\vartheta,\varphi)\,, \qquad (0 \le \vartheta \le \pi\,; \quad 0 \le \varphi \le 2\pi)\ , \tag{2.2}$$

where $R(\vartheta,\varphi)$ is a piece-wise C^2 function in $[0,\pi]\times[0,2\pi]$. We suppose the domain $\mathcal{D}$ satisfies

$$0 < A \le r \le R(\vartheta,\varphi)\,,$$

and therefore $\displaystyle\min_{(\vartheta,\varphi)\in[0,\pi]\times[0,2\pi]} R(\vartheta,\varphi) > 0$.

We introduce the stretched radius ρ such that

$$r = \rho\, R(\vartheta,\varphi)\,, \tag{2.3}$$

and the curvilinear (i.e. stretched) co-ordinates ρ,ϑ,φ, in the space x,y,z,

$$x = \rho\, R(\vartheta,\varphi)\,\cos\varphi\sin\vartheta\,,\ y = \rho\, R(\vartheta,\varphi)\,\sin\varphi\sin\vartheta\,,\ z = \rho\, R(\vartheta,\varphi)\,\cos\vartheta\,. \tag{2.4}$$

Therefore, $\mathcal{D}$ is obtained assuming $0 \le \vartheta \le \pi\,,\ 0 \le \varphi \le 2\pi\,,\ 0 \le \rho \le 1\,.$

Remark 12. Note that, in the stretched co-ordinate system the original domain $\mathcal{D}$ is transformed into the unit sphere, so that in this system we can use for the transformed Helmholtz equation all the classical techniques, including separation of variables.

We consider a $C^2(\mathcal{D})$ function $v(x,y,z) = v(r\cos\varphi\sin\vartheta, r\sin\varphi\sin\vartheta, r\cos\vartheta) = u(r,\vartheta,\varphi)$ and the Laplace operator in spherical co-ordinates

$$\Delta u = \frac{1}{r^2}\,\frac{\partial}{\partial r}\left(r^2\,\frac{\partial u}{\partial r}\right) + \frac{1}{r^2\sin\vartheta}\,\frac{\partial}{\partial\vartheta}\left(\sin\vartheta\,\frac{\partial u}{\partial\vartheta}\right) + \frac{1}{r^2\sin^2\vartheta}\,\frac{\partial^2 u}{\partial\varphi^2}\,. \tag{2.5}$$

We recall the expression of the Laplacian in the new stretched co-ordinate system ρ,ϑ,φ. Setting

$$U(\rho,\vartheta,\varphi) = u\left(\rho R(\vartheta,\varphi),\vartheta,\varphi\right)\ , \tag{2.6}$$

we find (denoting for shortness $R := R(\vartheta,\varphi)$) [3],

$$\begin{aligned}
\Delta u &= \frac{\partial^2 u}{\partial r^2} + \frac{2}{r}\,\frac{\partial u}{\partial r} + \frac{1}{r^2}\,\frac{\partial^2 u}{\partial\vartheta^2} + \frac{\cot\vartheta}{r^2}\,\frac{\partial u}{\partial\vartheta} + \frac{1}{r^2\sin^2\vartheta}\,\frac{\partial^2 u}{\partial\varphi^2} \\
&= \frac{1}{R^2}\left[1 + \frac{R_\vartheta^2}{R^2} + \frac{R_\varphi^2}{R^2\sin^2\vartheta}\right]\frac{\partial^2 U}{\partial\rho^2} \\
&+ \frac{1}{\rho R^2}\left[2\left(1 + \frac{R_\vartheta^2}{R^2} + \frac{R_\varphi^2}{R^2\sin^2\vartheta}\right) - \frac{1}{R}\left(R_\vartheta\cot\vartheta + R_{\vartheta\vartheta} + \frac{R_{\varphi\varphi}}{\sin^2\vartheta}\right)\right]\frac{\partial U}{\partial\rho} \\
&- 2\,\frac{R_\vartheta}{\rho R^3}\,\frac{\partial^2 U}{\partial\rho\partial\vartheta} - 2\,\frac{R_\varphi}{\rho R^3\sin^2\vartheta}\,\frac{\partial^2 U}{\partial\rho\partial\varphi} \\
&+ \frac{1}{\rho^2 R^2}\,\frac{\partial^2 U}{\partial\vartheta^2} + \frac{\cot\vartheta}{\rho^2 R^2}\,\frac{\partial U}{\partial\vartheta} + \frac{1}{\rho^2 R^2\sin^2\vartheta}\,\frac{\partial^2 U}{\partial\varphi^2}\,.
\end{aligned} \tag{2.7}$$

For $\rho = r\,,\ R(\vartheta,\varphi) \equiv 1$, we recover the Laplacian in spherical co-ordinates.

3 An equivalent formulation

For further computations, it is easier to change the spherical equation of $\partial\mathcal{D}$ by setting

$$\Upsilon := \Upsilon(\vartheta, \varphi) := \frac{1}{R(\vartheta, \varphi)} \qquad (0 \le \vartheta \le \pi\,; \quad 0 \le \varphi \le 2\pi). \tag{3.1}$$

The unit sphere is recovered whenever $\Upsilon(\vartheta, \varphi) \equiv 1$.

Using this spherical equation, the corresponding stretched co-ordinates ρ, ϑ, φ, in the space x, y, z, are given by

$$x = \frac{\rho}{\Upsilon(\vartheta, \varphi)} \cos\varphi \sin\vartheta\,, \; y = \frac{\rho}{\Upsilon(\vartheta, \varphi)} \sin\varphi \sin\vartheta\,, \; z = \frac{\rho}{\Upsilon(\vartheta, \varphi)} \cos\vartheta\,, \tag{3.2}$$

and assuming again, for shortness:

$$U(\rho, \vartheta, \varphi) = u\left(\frac{\rho}{\Upsilon(\vartheta, \varphi)}, \vartheta, \varphi\right),$$

the Laplacian becomes:

$$\begin{aligned}\Delta u = {} & \left(\Upsilon^2 + \Upsilon_\vartheta^2 + \frac{\Upsilon_\varphi^2}{\sin^2\vartheta}\right)\frac{\partial^2 U}{\partial\rho^2} + \frac{\Upsilon}{\rho}\left(2\Upsilon + \Upsilon_\vartheta \cot\vartheta + \Upsilon_{\vartheta\vartheta} + \frac{\Upsilon_{\varphi\varphi}}{\sin^2\vartheta}\right)\frac{\partial U}{\partial\rho} \\ & + \frac{2\Upsilon\Upsilon_\vartheta}{\rho}\frac{\partial^2 U}{\partial\rho\partial\vartheta} + \frac{2\Upsilon\Upsilon_\varphi}{\rho\sin^2\vartheta}\frac{\partial^2 U}{\partial\rho\partial\varphi} + \frac{\Upsilon^2}{\rho^2}\frac{\partial^2 U}{\partial\vartheta^2} \\ & + \frac{\Upsilon^2\cot\vartheta}{\rho^2}\frac{\partial U}{\partial\vartheta} + \frac{\Upsilon^2}{\rho^2\sin^2\vartheta}\frac{\partial^2 U}{\partial\varphi^2}\,.\end{aligned} \tag{3.3}$$

For $\rho = r$, $\Upsilon(\vartheta, \varphi) \equiv 1$, we find again the Laplacian in spherical co-ordinates.

4 Applications to the Helmholtz equation

Consider the Dirichlet problem for the Helmholtz equation

$$\begin{cases} \Delta u(r, \vartheta, \varphi) + \kappa^2 u(r, \vartheta, \varphi) = 0\,, & r < R(\vartheta, \varphi) \quad (0 \le \vartheta \le \pi\,,\ 0 \le \varphi < 2\pi)\,, \\ u(r, \vartheta, \varphi) = f(\vartheta, \varphi)\,, & r = R(\vartheta, \varphi) \quad (0 \le \vartheta \le \pi\,,\ 0 \le \varphi < 2\pi)\,. \end{cases} \tag{4.1}$$

We prove the following result

Theorem 4.1. – *Let*

$$f(\vartheta, \varphi) = \sum_{n=0}^{+\infty}\sum_{m=0}^{n} P_n^m(\cos\vartheta)\left(\alpha_{n,m}\cos m\varphi + \beta_{n,m}\sin m\varphi\right)\,, \tag{4.2}$$

where

$$\left\{\begin{matrix}\alpha_{n,m} \\ \beta_{n,m}\end{matrix}\right\} = \epsilon_m \frac{2n+1}{4\pi}\,\frac{(n-m)!}{(n+m)!}\int_0^{2\pi}\!\!\int_0^{\pi} f(\vartheta, \varphi) P_n^m(\cos\vartheta)\left\{\begin{matrix}\cos m\varphi \\ \sin m\varphi\end{matrix}\right\}\sin\vartheta d\vartheta\, d\varphi\,, \tag{4.3}$$

$\epsilon_m = \begin{cases} 1\,, & m=0 \\ 2\,, & m\neq 0 \end{cases}$ *, and P_n^m are the associated Legendre functions of the first kind* (see [9]).

Then, the solution of the interior Dirichlet problem for the Helmholtz equation *can be represented as*

$$u(r,\vartheta,\varphi) = \sum_{n=0}^{+\infty}\sum_{m=0}^{n} j_n(\kappa r) P_n^m(\cos\vartheta)\left(a_{n,m}\cos m\varphi + b_{n,m}\sin m\varphi\right)\,, \tag{4.4}$$

where the coefficients $a_{n,m}, b_{n,m}$ *can be found by solving the infinite linear system*

$$\sum_{n=0}^{+\infty}\sum_{m=0}^{n} \begin{bmatrix} X^{+}_{n,m,h,k} & Y^{+}_{n,m,h,k} \\ X^{-}_{n,m,h,k} & Y^{-}_{n,m,h,k} \end{bmatrix} \cdot \begin{bmatrix} a_{n,m} \\ b_{n,m} \end{bmatrix} = \begin{bmatrix} \alpha_{h,k} \\ \beta_{h,k} \end{bmatrix}$$

$$(h \in \mathbf{N_0}\,,\ k = 0,1,\ldots,h)\,, \tag{4.5}$$

where

$$X^{\pm}_{n,m,h,k} = \epsilon_k \frac{2h+1}{4\pi}\frac{(h-k)!}{(h+k)!}\int_0^{2\pi}\!\!\int_0^{\pi} j_n\left[\kappa R(\vartheta,\varphi)\right] P_n^m(\cos\vartheta) P_h^k(\cos\vartheta)\cos m\varphi \begin{Bmatrix}\cos k\varphi \\ \sin k\varphi\end{Bmatrix} \cdot \sin\vartheta\, d\vartheta d\varphi\,,$$

$$Y^{\pm}_{n,m,h,k} = \epsilon_k \frac{2h+1}{4\pi}\frac{(h-k)!}{(h+k)!}\int_0^{2\pi}\!\!\int_0^{\pi} j_n\left[\kappa R(\vartheta,\varphi)\right] P_n^m(\cos\vartheta) P_h^k(\cos\vartheta)\sin m\varphi \begin{Bmatrix}\cos k\varphi \\ \sin k\varphi\end{Bmatrix} \cdot \sin\vartheta\, d\vartheta d\varphi\,.$$

Proof. Recalling Remark 1, elementary solutions of the problem (4.1) can be searched in the form

$$u(r,\vartheta,\varphi) = U\left(\frac{\rho}{R(\vartheta,\varphi)}\,,\vartheta,\varphi\right) = P(r)\Theta(\vartheta)\Phi(\varphi)\,. \tag{4.6}$$

Substituting into the Helmholtz equation we find that the functions P, Θ, Φ must satisfy the ordinary differential equations

$$\begin{cases} r^2\,\dfrac{d^2P}{dr^2} + 2r\,\dfrac{dP}{dr} + \left(\kappa^2 r^2 - \lambda^2\right)P = 0\,, \\[2ex] \dfrac{1}{\sin\vartheta}\,\dfrac{d}{d\vartheta}\left(\sin\vartheta\,\dfrac{d\Theta}{d\vartheta}\right) + \left(\lambda^2 - \dfrac{\mu^2}{\sin^2\vartheta}\right)\Theta = 0\,, \\[2ex] \dfrac{d^2\Phi}{d\varphi^2} + \mu^2\Phi = 0\,, \end{cases} \tag{4.7}$$

and therefore, by using very classical results, we find

$$\mu = m \in \mathbf{Z}\,,$$

$$\lambda^2 = n(n+1)\,, \qquad n \in \mathbf{N_0}$$

$$\Phi(\varphi) = A_m \cos m\varphi + B_m \sin m\varphi \qquad (A_m, B_m \text{ arbitrary constants}),$$

and consequently

$$P(r) = C_n j_n(\kappa r) \qquad (C_n \text{ arbitrary constant}),$$

where

$$j_n(z) = \sqrt{\frac{\pi}{2z}} J_{n+\frac{1}{2}}(z) = (2z)^n \sum_{m=0}^{\infty} \frac{(-1)^m (n+m)!}{m!\,[2(n+m)+1]!}\, z^{2m}$$

are the spherical Bessel functions of the first kind [9].
Furthermore,

$$\Theta(\vartheta) = D_{n,m} P_n^m(\cos\vartheta) \qquad (d_{n,m} \text{ arbitrary constant}),$$

where

$$P_n^m(\eta) = (-1)^m (1-\eta^2)^{m/2} \frac{d^m P_n(\eta)}{d\eta^m} = (-1)^m \frac{(1-\eta^2)^{m/2}}{2^n\, n!} \frac{d^{n+m}(\eta^2-1)^n}{d\eta^{n+m}}\,.$$

Therefore a general solution of the Helmholtz equation can be written in the form

$$u(r,\vartheta,\varphi) = \sum_{n=0}^{+\infty} \sum_{m=0}^{n} j_n(\kappa r) P_n^m(\cos\vartheta)\,(a_{n,m}\cos m\varphi + b_{n,m}\sin m\varphi)\,. \tag{4.8}$$

Imposing the boundary condition

$$\begin{aligned} f(\vartheta,\varphi) &= U(1,\vartheta,\varphi) = u\,[R(\vartheta,\varphi),\vartheta,\varphi] \\ &= \sum_{n=0}^{+\infty} \sum_{m=0}^{n} j_n\,[\kappa R(\vartheta,\varphi)]\, P_n^m(\cos\vartheta)\,(a_{n,m}\cos m\varphi + b_{n,m}\sin m\varphi)\,, \end{aligned} \tag{4.9}$$

we find the unknown constants $a_{n,m}, b_{n,m}$ by solving the system (4.5). ■

Remark 13. Note that, assuming the unessential condition $R(\vartheta,\varphi) \le M < 1$, $\forall(\vartheta,\varphi) \in [0,\pi] \times [0,2\pi]$, the system (4.5) can be solved in an approximate way by considering the corresponding finite system where $n = 0,1,\ldots,N$, and $h = 0,1,\ldots,N$, $k = 0,1,\ldots,h$, and the solution is convergent when $N \to +\infty$.

Remark 14. Note that the above considerations hold whenever the function $R(\vartheta,\varphi)$ is a piecewise continuous function, and if the boundary data are given by square integrable functions, not necessarily continuous, so that the relevant coefficients $\alpha_{h,k}, \beta_{h,k}$ in equation (4.3) are finite.

In a similar way we can treat the *exterior problem* subject to the Sommerfeld radiation condition

$$\lim r \left[\frac{\partial}{\partial r} u(r,\vartheta,\varphi) - i\kappa u(r,\vartheta,\varphi)\right] = 0\,.$$

The only difference is that in solution (4.4) the spherical Bessel function of the first kind $j_n(z)$ must be replaced by the spherical Bessel function of the third kind $h^{(1)}(z)$, defined by [10]

$$h_n^{(1)}(z) = \sqrt{\frac{\pi}{2z}}\, H^{(1)}_{n+\frac{1}{2}}(z) = \sqrt{\frac{\pi}{2z}} \left[J_{n+\frac{1}{2}}(z) + iY_{n+\frac{1}{2}}(z)\right]\,.$$

5 Numerical examples

In the following examples we assume for the boundary $\partial\mathcal{D}$ a general spherical equation of the type

$$R(\vartheta,\varphi) = c\left[\left|\frac{\sin\frac{p\vartheta}{2}\cos\frac{q\varphi}{4}}{\gamma_1}\right|^{\nu_1} + \left|\frac{\sin\frac{p\vartheta}{2}\sin\frac{q\varphi}{4}}{\gamma_2}\right|^{\nu_2} + \left|\frac{\cos\frac{p\vartheta}{2}}{\gamma_3}\right|^{\nu_3}\right]^{-1/\nu_0}, \tag{5.1}$$

($p, q, \gamma_1, \gamma_2, \gamma_3, \nu_0, \nu_1, \nu_2, \nu_3$ integral numbers), extending to the three-dimensional case the curves introduced by J. Gielis [7]. Moreover, let $F(x, y, z)$ denote the function representing boundary values. Under such assumptions, the following expression results

$$f(\vartheta,\varphi) = F\left(R(\vartheta,\varphi)\cos\varphi\sin\vartheta, R(\vartheta,\varphi)\sin\varphi\sin\vartheta, R(\vartheta,\varphi)\cos\vartheta\right). \tag{5.2}$$

In numerical experiments, computed by using Mathematica©, we assume different values of the nine parameters $p, q, \gamma_1, \gamma_2, \gamma_3, \nu_0, \nu_1, \nu_2, \nu_3$, obtaining very different shapes for the considered domain, including ellipsoids, Lamé-type domains (also called *Superellipsoids*), ovaloids, (p, q)-fold symmetric figures, and so on. We introduced furthermore an extra parameter c, in order to ensure the convergence condition $\max\limits_{(\vartheta,\varphi)\in[0,\pi]\times[0,2\pi]} R(\vartheta,\varphi) \le M < 1$. We emphasize that almost all three-dimensional normal-polar domains are described (or at least approximated in a close way) by the above mentioned surfaces.

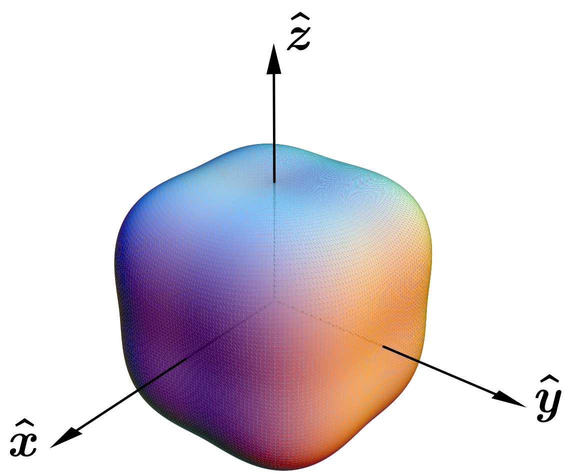

Figure 1: *Tridimensional view of the domain* $\mathcal{D}$ *obtained by assuming in* (5.1) $\gamma_1 = \gamma_2 = \gamma_3 = 1$, $p = 2$, $q = 4$, $\nu_0 = 2$, $\nu_1 = \nu_2 = \nu_3 = 3$. *The parameter* c *has been set in order to ensure the condition* $\max\limits_{(\vartheta,\varphi)\in[0,\pi]\times[0,2\pi]} R(\vartheta,\varphi) = 1$.

In particular, to assess the performances of the proposed algorithm in terms of numerical accuracy and convergence rate, the relative boundary error has been evaluated as follows

$$e_N = \frac{\|U_N(1,\vartheta,\varphi) - f(\vartheta,\varphi)\|}{\|f(\vartheta,\varphi)\|}, \tag{5.3}$$

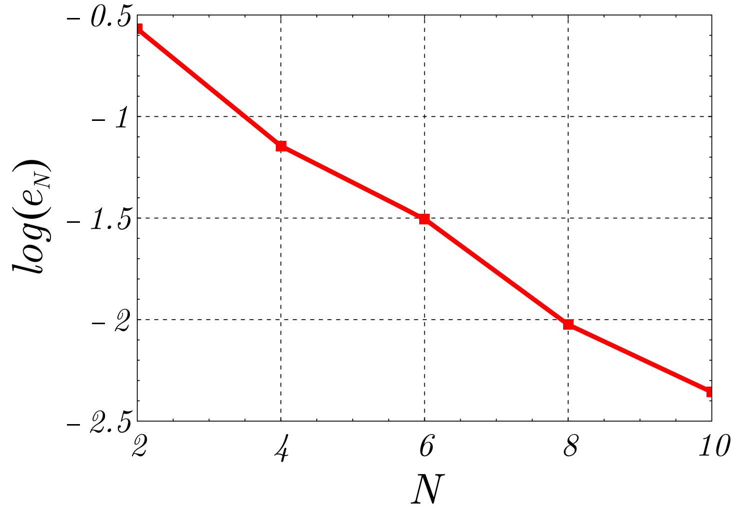

Figure 2: *Relative boundary error* e_N *as function of the number* N *of terms in the expansion series* (5.4) *approximating the solution of the interior Dirichlet problem for the Helmholtz equation in the star-like domain* $\mathcal{D}$ *described by the spherical equation* (5.1) *with* $\gamma_1 = \gamma_2 = \gamma_3 = 1$, $p = 2$, $q = 4$, $\nu_0 = 2$, $\nu_1 = \nu_2 = \nu_3 = 3$.

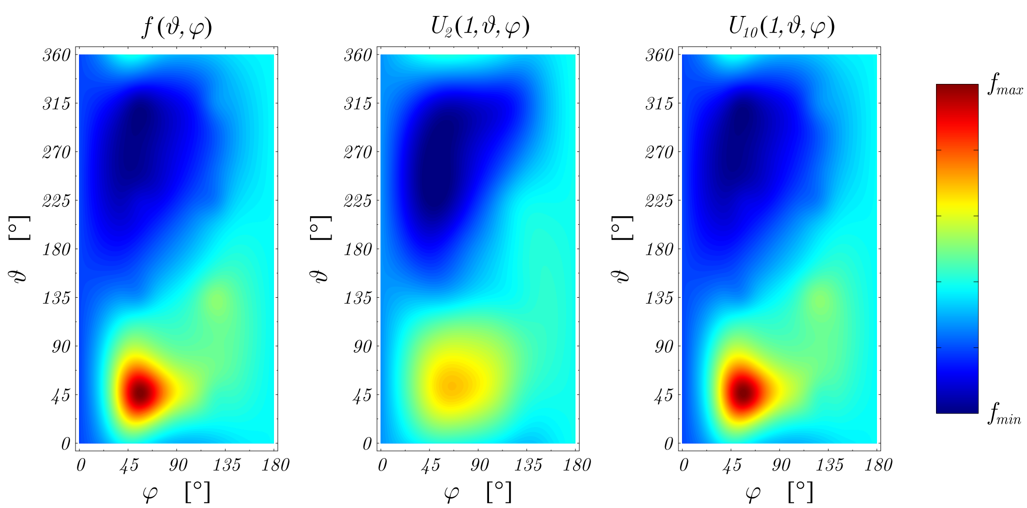

Figure 3: *Angular behavior of the* $N-th$ *partial sum* $U_N(1, \vartheta, \varphi)$ *of the spherical harmonics series approximating the solution of the interior Dirichlet problem for the Helmholtz equation in the star-like domain* $\mathcal{D}$ *described by the spherical equation* (5.1) *with* $\gamma_1 = \gamma_2 = \gamma_3 = 1$, $p = 2$, $q = 4$, $\nu_0 = 2$, $\nu_1 = \nu_2 = \nu_3 = 3$.

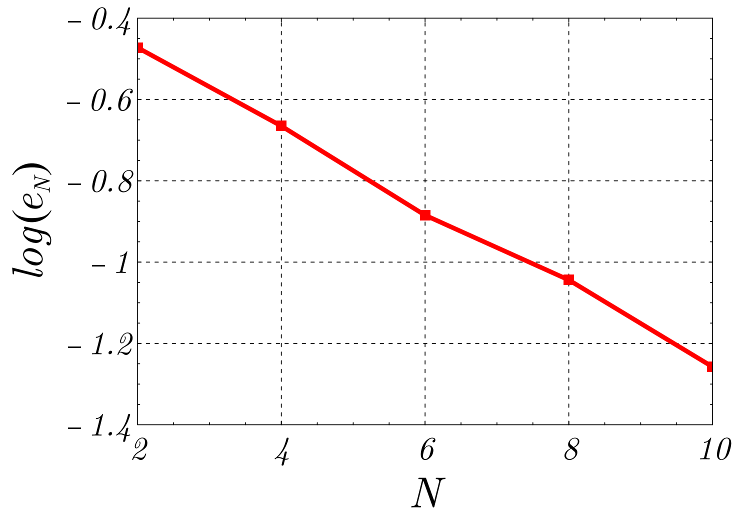

Figure 4: *Relative boundary error* e_N *as function of the number* N *of terms in the expansion series approximating the solution of the exterior Dirichlet problem for the Helmholtz equation in the star-like domain* $\mathcal{D}$ *described by the spherical equation* (5.1) *with* $\gamma_1 = \gamma_2 = \gamma_3 = 1$, $p = 2$, $q = 4$, $\nu_0 = 2$, $\nu_1 = \nu_2 = \nu_3 = 3$.

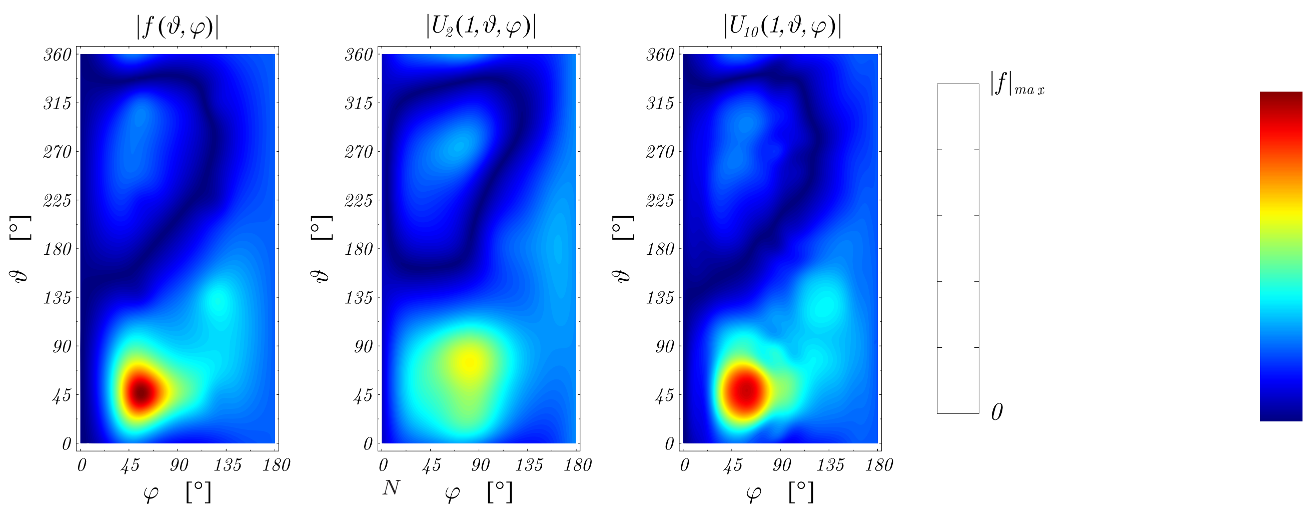

Figure 5: *Angular behavior of the* $N-th$ *partial sum* $U\ \ (1,\vartheta,\varphi)$ *of the spherical harmonics series approximating the solution of the exterior Dirichlet problem for the Helmholtz equation in the star-like domain* $\mathcal{D}$ *described by the spherical equation* (5.1) *with* $\gamma_1 = \gamma_2 = \gamma_3 = 1$, $p = 2$, $q = 4$, $\nu_0 = 2$, $\nu_1 = \nu_2 = \nu_3 = 3$.

where $\|\cdot\|$ denotes the usual $L^2(\partial\mathcal{D})$ norm, and

$$U_N(\rho,\vartheta,\varphi) = \sum_{n=0}^{N}\sum_{m=0}^{n} j_n\left[\kappa\rho R(\vartheta,\varphi)\right] P_n^m(\cos\vartheta)\left(A_{n,m}\cos m\varphi + B_{n,m}\sin m\varphi\right), \qquad (5.4)$$

is the N-th partial sum of the approximating spherical harmonics series (4.8).

5.1 Example 1 – Interior problem

By assuming in (5.1) $\gamma_1 = \gamma_2 = \gamma_3 = 1$, $p = 2$, $q = 4$, $\nu_0 = 2$, $\nu_1 = \nu_2 = \nu_3 = 3$, the domain $\mathcal{D}$ features the shape depicted in Fig. 1.

Let $F(x,y,z) = x^3y^3z^3 + e^{x+y+z} - x + 2y - 3z$ be the function representing boundary values. Then, the relative boundary error e_N as function of the number N of terms in the relavant expansion (5.4) exhibits the behavior shown in Fig. 2.

Finally, the maps in Fig. 3 clearly show the convergence rate of the approximating sequence of functions $U_N(1,\vartheta,\varphi)$ to the boundary values $f(\vartheta,\varphi)$.

5.2 Example 2 – Exterior problem

Let us now focus the attention on the exterior Dirichlet problem for the Helmholtz equation in the star-like domain complementary to that considered in the previous example, under the hypothesis that the boundary values are still described by the function $F(x,y,z) = x^3y^3z^3 + e^{x+y+z} - x + 2y - 3z$. Then, the relative boundary error e_N as function of the number N of terms in the expansion series approximating the solution of the problem exhibits the behavior shown in Fig. 4.

Finally, the maps in Fig. 5 clearly show the convergence rate of the approximating sequence of functions $U_N(1,\vartheta,\varphi)$ to the boundary values $f(\vartheta,\varphi)$.

Remark 15. – If the boundary values have wide oscillations, it is necessary to increase the number N of terms in the relevant Fourier expansion, in order to obtain better results.

Remark 16. – The L^2 norm of the difference between the exact solution and its approximate values is always vanishing in the interior (exterior) of the considered domain, and generally small on the boundary. Point-wise convergence seems to be true on the whole boundary, with only exception of a set of measure zero, corresponding to singular points for the function or its derivative. In these points oscillations of the approximate solution, recalling the classical Gibbs phenomenon, usually appear.

6 Conclusion

It seems that the use of stretched co-ordinate system, reducing every starlike domain to a circle, allow to use the classical Fourier methods to a very large class of domains, permitting to find solutions in a closed form, and to avoid some more cumbersome techniques such as the finite difference methods or the finite element method (FEM) [11], since it is possible to use only quadrature rules and solution of linear systems.

Acknowledgments - This article was conclude under a grant by Italian PRIN/2006 Cap. 7320.

References

[1] P. Natalini, P.E. Ricci, The Laplacian in stretched polar co-ordinates and Applications, *Proceedings ISAAC Conference on "Complex Analysis, Partial Differential Equations and Mechanics of Continua", dedicated to the Centenary of Ilia Vekua* (to appear).

[2] P. Natalini, R. Patrizi, P.E. Ricci, The Dirichlet problem for the Laplace equation in a starlike domain of a Riemann surface, Numer. Algorithms, (to appear).

[3] D. Caratelli, P.E. Ricci, *The Dirichlet problem for the Laplace equation in a starlike domain*, Proc. "The 2008 International Conference on Scientific Computing", Las Vegas, July 14-17, 2008, 160–166.

[4] D. Caratelli, B. Germano, M.X. He, P.E. Ricci, The Dirichlet problem for the Laplace equation in a cylindrical domain, (in progress).

[5] G.P. Tolstov, *Fourier Series*, Transl. from Russian by R.A. Silverman, Dover Publ. Inc., New York, 1962.

[6] N.N. Lebedev, Special Functions and Their Applications, Dover Publ. Inc., New York, 1972.

[7] J. Gielis, A generic geometric transformation that unifies a wide range of natural and abstract shapes, *Amer. J. Botany*, **90**, (2003), 333–338.

[8] L. Carleson, On convergence and growth of partial sums of Fourier series. *Acta Math.*, **116** (1966), 135–157.

[9] L.C. Andrews, *Special Functions of Mathematics for Engineers*, Oxford Univ. Press, Oxford, New York, 1998.

[10] M. Abramowitz, I.A. Stegun, eds., *Handbook of Mathematical Functions with Formulas, Graphs, and Mathematical Tables*, Dover Publ. Inc., New York, 1972.

[11] A. Bondeson, T. Rylander, P. Ingelstrom, *Computational Electromagnetics*, Springer Science, Texts in Applied Mathematics, New York, 2005.

Appendix Mathematica© programs

by **Diego Caratelli**

Delft University of Technology, IRCTR,
Mekelweg, 4, 2628 CD, Delft, the Netherlands
e-mail: d.caratelli@tudelft.nl

```
Off[General::spell]
Off[General::spell1]
Off[NIntegrate::ncvb]
Off[NIntegrate::tmap]
Off[NIntegrate::ploss]
Off[NIntegrate::slwcon]
Off[NIntegrate::eincr]
```

red[x_]:=Which $\left[x \leq \frac{3}{8}, 0, \left(x > \frac{3}{8}\right) \&\& \left(x \leq \frac{5}{8}\right),\right.$
$\left. 4x - \frac{3}{2}, \left(x > \frac{5}{8}\right) \&\& \left(x \leq \frac{7}{8}\right), 1, x > \frac{7}{8}, -4x + \frac{9}{2}\right]$
green[x_]:=Which $\left[x \leq \frac{1}{8}, 0, \left(x > \frac{1}{8}\right) \&\& \left(x \leq \frac{3}{8}\right),\right.$
$4x - \frac{1}{2}, \left(x > \frac{3}{8}\right) \&\& \left(x \leq \frac{5}{8}\right), 1, \left(x > \frac{5}{8}\right) \&\& \left(x \leq \frac{7}{8}\right),$
$\left. -4x + \frac{7}{2}, x > \frac{7}{8}, 0\right]$
blue[x_]:=Which $\left[x \leq \frac{1}{8}, 4x + \frac{1}{2}, \left(x > \frac{1}{8}\right) \&\& \left(x \leq \frac{3}{8}\right),\right.$
$\left. 1, \left(x > \frac{3}{8}\right) \&\& \left(x \leq \frac{5}{8}\right), -4x + \frac{5}{2}, x > \frac{5}{8}, 0\right]$
JetFunction[x_]:=RGBColor[red[x], green[x], blue[x]]

```
TextFont:="Euclid"
TextPointSize:=24
LabelPointSize:=32
```

γ_1:=1
γ_2:=1
γ_3:=1
m:=2
n:=4
ν_0:=2
ν_1:=3
ν_2:=3
ν_3:=3
$r[\theta\_, \varphi\_, \mathrm{K}\_]$:=

$$K\left(\mathrm{Abs}\left[\frac{\mathrm{Sin}\left[\frac{m\theta}{2}\right]\mathrm{Cos}\left[\frac{n\varphi}{4}\right]}{\gamma_1}\right]^{\nu_1} + \mathrm{Abs}\left[\frac{\mathrm{Sin}\left[\frac{m\theta}{2}\right]\mathrm{Sin}\left[\frac{n\varphi}{4}\right]}{\gamma_2}\right]^{\nu_2} + \mathrm{Abs}\left[\frac{\mathrm{Cos}\left[\frac{m\theta}{2}\right]}{\gamma_3}\right]^{\nu_3}\right)^{-\frac{1}{\nu_0}}$$

$$\mathcal{K} = \frac{1}{\mathrm{NMaximize}[r[\theta,\varphi,1],\{\theta,\varphi\}]_{[[1]]}};$$

X:=1.45
Y:=1.3
Z:=1.25
ReferenceSystem =
Graphics3D[{Black, EdgeForm[Black],Thickness[0.0025], EdgeForm[Thickness[0.0025]],
Line $\left[\left\{\left\{-\frac{X}{8}, 0, 0\right\}, \{X, 0, 0\}\right\}\right]$,Polygon $\left[\left\{\left\{X, -\frac{1}{50}\text{Max}[X, Y, Z], 0\right\}\right.\right.$,
$\left\{X, \frac{1}{50}\text{Max}[X, Y, Z], 0\right\}, \left\{X + \frac{1}{12}\text{Max}[X, Y, Z], 0, 0\right\}\}]$,
Line $\left[\left\{\left\{0, -\frac{Y}{8}, 0\right\}, \{0, Y, 0\}\right\}\right]$,Polygon $\left[\left\{\left\{-\frac{1}{50}\text{Max}[X, Y, Z], Y, 0\right\}\right.\right.$,
$\left\{\frac{1}{50}\text{Max}[X, Y, Z], Y, 0\right\}, \left\{0, Y + \frac{1}{12}\text{Max}[X, Y, Z], 0\right\}\}]$,
Line $\left[\left\{\left\{0, 0, -\frac{Z}{8}\right\}, \{0, 0, Z\}\right\}\right]$,Polygon $\left[\left\{\left\{-\frac{\text{Max}[X,Y,Z]}{50\sqrt{2}}, \frac{\text{Max}[X,Y,Z]}{50\sqrt{2}}, Z\right\}\right.\right.$,
$\left\{\frac{\text{Max}[X,Y,Z]}{50\sqrt{2}}, -\frac{\text{Max}[X,Y,Z]}{50\sqrt{2}}, Z\right\}, \left\{0, 0, Z + \frac{1}{12}\text{Max}[X, Y, Z]\right\}\}]$,
Text [Style ["$\hat{x}$", FontFamily → TextFont, FontSlant → Italic, FontWeight → Bold,
FontSize → LabelPointSize], $\left\{X + \frac{1}{10}\text{Max}[X, Y, Z], -\frac{1}{15}\text{Max}[X, Y, Z], 0\right\}$] ,
Text [Style ["$\hat{y}$", FontFamily → TextFont, FontSlant → Italic, FontWeight → Bold,
FontSize → LabelPointSize], $\left\{-\frac{1}{15}\text{Max}[X, Y, Z], Y + \frac{1}{10}\text{Max}[X, Y, Z], 0\right\}$] ,
Text [Style ["$\hat{z}$", FontFamily → TextFont, FontSlant → Italic, FontWeight → Bold,
FontSize → LabelPointSize], $\left\{-\frac{\text{Max}[X,Y,Z]}{15\sqrt{2}}, \frac{\text{Max}[X,Y,Z]}{15\sqrt{2}},\right.$
$Z + \frac{1}{10}\text{Max}[X, Y, Z]\}]\}$, Lighting → None,Boxed → False, AspectRatio → Automatic,
DisplayFunction → Identity];

$\mathcal{R}[\theta\_, \varphi\_]$:=$r[\theta, \varphi, \mathcal{K}]$

f[x_, y_, z_]:=$e^{x+iy+z} - x + 2iy - 3z$
$f[\theta\_, \varphi\_]$:=$f[\mathcal{R}[\theta, \varphi]\text{Sin}[\theta]\text{Cos}[\varphi]$,
$\mathcal{R}[\theta, \varphi]\text{Sin}[\theta]\text{Sin}[\varphi], \mathcal{R}[\theta, \varphi]\text{Cos}[\theta]]$

M_θ:=50
M_φ:=100
$\Delta\theta = \frac{\pi}{M_\theta}$;
$\Delta\varphi = \frac{2\pi}{M_\varphi}$;

$\mathcal{P}_{\text{i\_,j\_}} = \{\mathcal{R}[i\Delta\theta, j\Delta\varphi]\text{Sin}[i\Delta\theta]\text{Cos}[j\Delta\varphi], \mathcal{R}[i\Delta\theta, j\Delta\varphi]\text{Sin}[i\Delta\theta]\text{Sin}[j\Delta\varphi]$,
$\mathcal{R}[i\Delta\theta, j\Delta\varphi]\text{Cos}[i\Delta\theta]\}$;

$v =$ Table $\left[\text{Abs}\left[N\left[f\left[\left(i - \frac{1}{2}\right)\Delta\theta, \left(j - \frac{1}{2}\right)\Delta\varphi\right]\right]\right], \{i, M_\theta\}, \{j, M_\varphi\}\right]$;

$\mathcal{M} = \text{Max}[v]$;

Clipping[$\mathfrak{v}$_]:=Which $\left[\mathfrak{v} < m, 0, m \le \mathfrak{v} \le \mathcal{M}, \frac{\mathfrak{v}-m}{\mathcal{M}-m}, \mathfrak{v} > \mathcal{M}, 1\right]$

FPlot = Graphics3D[Table $\left[\left\{\text{EdgeForm}[], \text{JetFunction}\left[\text{Clipping}\left[v_{[[i,j]]}\right]\right]\right.\right.$,
Polygon $[\{\mathcal{P}_{i-1,j}, \mathcal{P}_{i,j}, \mathcal{P}_{i,j-1}, \mathcal{P}_{i-1,j-1}\}]\}, \{i, M_\theta\}, \{j, M_\varphi\}]$, Lighting → Automatic,
Boxed → False, AspectRatio → Automatic,DisplayFunction → Identity];

F = Show[FPlot, ReferenceSystem, PlotRange → All,ViewPoint → {2.0, 1.5, 1.5},
DisplayFunction → $DisplayFunction]

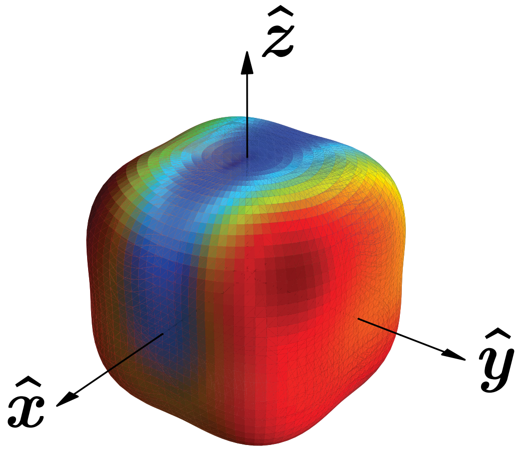

$\varepsilon_{\mathfrak{m}\_}$:=If$[\mathfrak{m} == 0, 1, 2]$

$\alpha_{\mathfrak{n}\_,\mathfrak{m}\_}$:=$\varepsilon_{\mathfrak{m}} \frac{2\mathfrak{n}+1}{4\pi} \frac{(\mathfrak{n}-\mathfrak{m})!}{(\mathfrak{n}+\mathfrak{m})!}$NIntegrate[$f[\theta, \varphi]$LegendreP[$\mathfrak{n}, \mathfrak{m}$, Cos[$\theta$]]
Cos[$\mathfrak{m}\varphi$]Sin[θ], $\{\theta, 0, \pi\}$, $\{\varphi, 0, 2\pi\}$,Method $\rightarrow$ MultiDimensional, AccuracyGoal $\rightarrow$ 6,
PrecisionGoal $\rightarrow$ 6]
$\beta_{\mathfrak{n}\_,\mathfrak{m}\_}$:=$\varepsilon_{\mathfrak{m}} \frac{2\mathfrak{n}+1}{4\pi} \frac{(\mathfrak{n}-\mathfrak{m})!}{(\mathfrak{n}+\mathfrak{m})!}$NIntegrate[$f[\theta, \varphi]$LegendreP[$\mathfrak{n}, \mathfrak{m}$, Cos[$\theta$]]
Sin[$\mathfrak{m}\varphi$]Sin[θ], $\{\theta, 0, \pi\}$, $\{\varphi, 0, 2\pi\}$,Method $\rightarrow$ MultiDimensional, AccuracyGoal $\rightarrow$ 6,
PrecisionGoal $\rightarrow$ 6]

$\chi[\mathfrak{n}\_]$:=$\mathfrak{n}$
$\xi[\mathfrak{n}\_, \mathfrak{m}\_, \theta\_, \varphi\_]$:=$\mathcal{R}[\theta, \varphi]^{\chi[\mathfrak{n}]}$LegendreP[$\mathfrak{n}, \mathfrak{m}$, Cos[$\theta$]]Cos[$\mathfrak{m}\varphi$]
$\eta[\mathfrak{n}\_, \mathfrak{m}\_, \theta\_, \varphi\_]$:=$\mathcal{R}[\theta, \varphi]^{\chi[\mathfrak{n}]}$LegendreP[$\mathfrak{n}, \mathfrak{m}$, Cos[$\theta$]]Sin[$\mathfrak{m}\varphi$]

$\mathcal{X}^{+}_{\mathfrak{n}\_,\mathfrak{m}\_,\mathfrak{h}\_,\mathfrak{k}\_}$:=$\varepsilon_{\mathfrak{k}} \frac{2\mathfrak{h}+1}{4\pi} \frac{(\mathfrak{h}-\mathfrak{k})!}{(\mathfrak{h}+\mathfrak{k})!}$NIntegrate[$\xi[\mathfrak{n}, \mathfrak{m}, \theta, \varphi]$LegendreP[$\mathfrak{h}, \mathfrak{k}$, Cos[$\theta$]]
Cos[$\mathfrak{k}\varphi$]Sin[θ], $\{\theta, 0, \pi\}$, $\{\varphi, 0, 2\pi\}$,Method $\rightarrow$ MultiDimensional, AccuracyGoal $\rightarrow$ 6,
PrecisionGoal $\rightarrow$ 6]
$\mathcal{X}^{-}_{\mathfrak{n}\_,\mathfrak{m}\_,\mathfrak{h}\_,\mathfrak{k}\_}$:=$\varepsilon_{\mathfrak{k}} \frac{2\mathfrak{h}+1}{4\pi} \frac{(\mathfrak{h}-\mathfrak{k})!}{(\mathfrak{h}+\mathfrak{k})!}$NIntegrate[$\xi[\mathfrak{n}, \mathfrak{m}, \theta, \varphi]$LegendreP[$\mathfrak{h}, \mathfrak{k}$, Cos[$\theta$]]
Sin[$\mathfrak{k}\varphi$]Sin[θ], $\{\theta, 0, \pi\}$, $\{\varphi, 0, 2\pi\}$,Method $\rightarrow$ MultiDimensional, AccuracyGoal $\rightarrow$ 6,
PrecisionGoal $\rightarrow$ 6]
$\mathcal{Y}^{+}_{\mathfrak{n}\_,\mathfrak{m}\_,\mathfrak{h}\_,\mathfrak{k}\_}$:=$\varepsilon_{\mathfrak{k}} \frac{2\mathfrak{h}+1}{4\pi} \frac{(\mathfrak{h}-\mathfrak{k})!}{(\mathfrak{h}+\mathfrak{k})!}$NIntegrate[$\eta[\mathfrak{n}, \mathfrak{m}, \theta, \varphi]$LegendreP[$\mathfrak{h}, \mathfrak{k}$, Cos[$\theta$]]
Cos[$\mathfrak{k}\varphi$]Sin[θ], $\{\theta, 0, \pi\}$, $\{\varphi, 0, 2\pi\}$,Method $\rightarrow$ MultiDimensional, AccuracyGoal $\rightarrow$ 6,
PrecisionGoal $\rightarrow$ 6]
$\mathcal{Y}^{-}_{\mathfrak{n}\_,\mathfrak{m}\_,\mathfrak{h}\_,\mathfrak{k}\_}$:=$\varepsilon_{\mathfrak{k}} \frac{2\mathfrak{h}+1}{4\pi} \frac{(\mathfrak{h}-\mathfrak{k})!}{(\mathfrak{h}+\mathfrak{k})!}$NIntegrate[$\eta[\mathfrak{n}, \mathfrak{m}, \theta, \varphi]$LegendreP[$\mathfrak{h}, \mathfrak{k}$, Cos[$\theta$]]
Sin[$\mathfrak{k}\varphi$]Sin[θ], $\{\theta, 0, \pi\}$, $\{\varphi, 0, 2\pi\}$,Method $\rightarrow$ MultiDimensional, AccuracyGoal $\rightarrow$ 6,
PrecisionGoal $\rightarrow$ 6]

$\mathcal{N}$:=4

$\mathfrak{E}$ = Flatten[Join[Table[Table $\Big[-\alpha_{\mathfrak{h},\mathfrak{k}} + \sum_{\mathfrak{n}=0}^{\mathcal{N}} \sum_{\mathfrak{m}=0}^{\mathfrak{n}} \mathfrak{a}_{\mathfrak{n},\mathfrak{m}} \mathcal{X}^{+}_{\mathfrak{n},\mathfrak{m},\mathfrak{h},\mathfrak{k}} +$
$\sum_{\mathfrak{n}=0}^{\mathcal{N}} \sum_{\mathfrak{m}=1}^{\mathfrak{n}} \mathfrak{b}_{\mathfrak{n},\mathfrak{m}} \mathcal{Y}^{+}_{\mathfrak{n},\mathfrak{m},\mathfrak{h},\mathfrak{k}}, \{\mathfrak{k}, 0, \mathfrak{h}\}\Big], \{\mathfrak{h}, 0, \mathcal{N}\}\Big]$,Table[
Table $\Big[-\beta_{\mathfrak{h},\mathfrak{k}} + \sum_{\mathfrak{n}=0}^{\mathcal{N}} \sum_{\mathfrak{m}=0}^{\mathfrak{n}} \mathfrak{a}_{\mathfrak{n},\mathfrak{m}} \mathcal{X}^{-}_{\mathfrak{n},\mathfrak{m},\mathfrak{h},\mathfrak{k}} +$

$\sum_{\mathfrak{n}=0}^{\mathcal{N}}\sum_{\mathfrak{m}=1}^{\mathfrak{n}}\mathfrak{b}_{\mathfrak{n},\mathfrak{m}}\mathcal{Y}^{-}_{\mathfrak{n},\mathfrak{m},\mathfrak{h},\mathfrak{k}},\{\mathfrak{k},1,\mathfrak{h}\}\Big],\{\mathfrak{h},0,\mathcal{N}\}\Big]\Big]\Big];$
$\mathfrak{NE}=\text{Length}[\mathfrak{E}];$

$\mathfrak{U}=\text{Flatten}\,[\text{Join}\,[\text{Table}\,[\text{Table}\,[\mathfrak{a}_{\mathfrak{n},\mathfrak{m}},\{\mathfrak{m},0,\mathfrak{n}\}],\{\mathfrak{n},0,\mathcal{N}\}],$
$\text{Table}\,[\text{Table}\,[\mathfrak{b}_{\mathfrak{n},\mathfrak{m}},\{\mathfrak{m},1,\mathfrak{n}\}],\{\mathfrak{n},0,\mathcal{N}\}]]];$
$\mathfrak{NU}=\text{Length}[\mathfrak{U}];$

$A=\text{Table}\left[\text{Coefficient}\left[\mathfrak{E}_{[[i]]},\mathfrak{U}_{[[j]]}\right],\{i,\mathfrak{NE}\},\{j,\mathfrak{NU}\}\right];$

$\text{EPS}{:=}10^{-6}$

$b=\text{Table}\left[\text{Chop}\left[-\mathfrak{E}_{[[i]]}+\sum_{j=1}^{\mathfrak{NU}}A_{[[i,j]]}\mathfrak{U}_{[[j]]},\text{EPS}\right],\{i,\mathfrak{NE}\}\right];$

$\mathfrak{C}=\text{Chop}[\text{PseudoInverse}[A].b,\text{EPS}];$
$\mathfrak{i}=1;$
$\text{For}[\mathfrak{N}=0,\mathfrak{N}\leq\mathcal{N},{+}{+}\mathfrak{N},$
$\text{For}[\mathfrak{M}=0,\mathfrak{M}\leq\mathfrak{N},{+}{+}\mathfrak{M},$
$\mathfrak{A}_{\mathfrak{N},\mathfrak{M}}=\mathfrak{C}_{[[\mathfrak{i}]]};$
$\mathfrak{i}{+}{=}1;$
]
]
$\text{For}[\mathfrak{N}=0,\mathfrak{N}\leq\mathcal{N},{+}{+}\mathfrak{N},$
$\text{For}[\mathfrak{M}=0,\mathfrak{M}\leq\mathfrak{N},{+}{+}\mathfrak{M},$
$\text{If}[\mathfrak{M}==0,$
$\mathfrak{B}_{\mathfrak{N},\mathfrak{M}}=0;$
,
$\mathfrak{B}_{\mathfrak{N},\mathfrak{M}}=\mathfrak{C}_{[[\mathfrak{i}]]};$
$\mathfrak{i}{+}{=}1;$
]
]
]

$\text{Print}\,[\text{"}[a_{n,m}]\text{="},\text{MatrixForm}\,[\text{Table}\,[\text{If}\,[\mathfrak{m}>\mathfrak{n},0,\mathfrak{A}_{\mathfrak{n},\mathfrak{m}}],\{\mathfrak{n},0,\mathcal{N}\},\{\mathfrak{m},0,\mathcal{N}\}]]];$
$\text{Print}\,[\text{"}[b_{n,m}]\text{="},\text{MatrixForm}\,[\text{Table}\,[\text{If}\,[\mathfrak{m}>\mathfrak{n}\|\mathfrak{m}==0,0,\mathfrak{B}_{\mathfrak{n},\mathfrak{m}}],\{\mathfrak{n},0,\mathcal{N}\},\{\mathfrak{m},0,\mathcal{N}\}]]];$

$$[a_{n,m}]=\begin{pmatrix}1.13064 & 0 & 0 & 0 & 0\\ -1.92057 & -0.0794314 & 0 & 0 & 0\\ 0.350663 & -0.353483 & 0.175331 & 0 & 0\\ 0.0568304 & -0.0730996 & 0.0349229 & -0.0110986 & 0\\ -0.0679669 & -0.00956732 & 0.00529085 & -0.00159455 & -0.0000266465\end{pmatrix}$$

$$[b_{n,m}]=\begin{pmatrix}0 & 0 & 0 & 0 & 0\\ 0 & -3.08014i & 0 & 0 & 0\\ 0 & -0.3536i & 0.1768i & 0 & 0\\ 0 & -0.0740652i & 0.03502i & -0.0123442i & 0\\ 0 & -0.00964811i & 0.00519477i & -0.00171394i & 0.000415244i\end{pmatrix}$$

$\mathcal{U}[\rho\_,\theta\_,\varphi\_]{:=}$
$\sum_{\mathfrak{n}=0}^{\mathcal{N}}\sum_{\mathfrak{m}=0}^{\mathfrak{n}}(\rho\mathcal{R}[\theta,\varphi])^{\chi[\mathfrak{n}]}\text{LegendreP}[\mathfrak{n},\mathfrak{m},\text{Cos}[\theta]](\mathfrak{A}_{\mathfrak{n},\mathfrak{m}}\text{Cos}[\mathfrak{m}\varphi]+\mathfrak{B}_{\mathfrak{n},\mathfrak{m}}\text{Sin}[\mathfrak{m}\varphi])$

$\mathcal{V}=\text{Table}\left[\text{Abs}\left[N\left[\mathcal{U}\left[1,\left(i-\tfrac{1}{2}\right)\Delta\theta,\left(j-\tfrac{1}{2}\right)\Delta\varphi\right]\right]\right],\{i,M_\theta\},\{j,M_\varphi\}\right];$

$\text{BVPlot} = \text{Graphics3D}[\text{Table}\left[\left\{\text{EdgeForm}[], \text{JetFunction}\left[\text{Clipping}\left[\mathcal{V}_{[[i,j]]}\right]\right],\right.\right.$
$\left.\text{Polygon}\left[\{\mathcal{P}_{i-1,j}, \mathcal{P}_{i,j}, \mathcal{P}_{i,j-1}, \mathcal{P}_{i-1,j-1}\}\right]\right\}, \{i, M_\theta\}, \{j, M_\varphi\}\right], \text{Lighting} \to \text{Automatic},$
$\text{Boxed} \to \text{False}, \text{AspectRatio} \to \text{Automatic}, \text{DisplayFunction} \to \text{Identity}];$

$\text{BV} = \text{Show}[\text{BVPlot}, \text{ReferenceSystem}, \text{PlotRange} \to \text{All}, \text{ViewPoint} \to \{2.0, 1.5, 1.5\},$
$\text{DisplayFunction} \to \$\text{DisplayFunction}]$

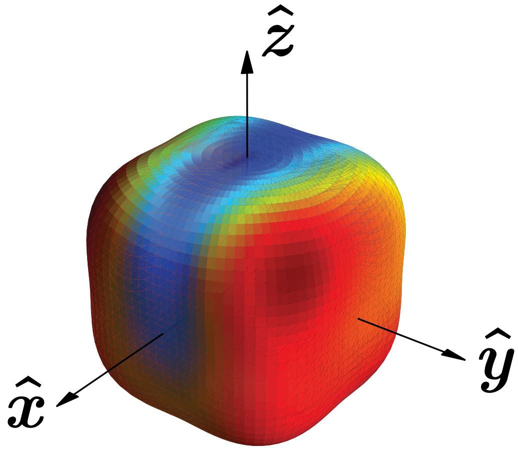

$e = 100 \times \left(\text{NIntegrate}\left[\text{Abs}[\mathcal{U}[1, \theta, \varphi] - f[\theta, \varphi]]^2 \mathcal{R}[\theta, \varphi] \text{Sin}[\theta], \ \{\theta, 0, \pi\}, \{\varphi, 0, 2\pi\},\right.\right.$
$\text{Method} \to \text{MultiDimensional}, \text{AccuracyGoal} \to 6, \text{PrecisionGoal} \to 6]/$
$\text{NIntegrate}\left[\text{Abs}[f[\theta, \varphi]]^2 \mathcal{R}[\theta, \varphi] \text{Sin}[\theta], \ \{\theta, 0, \pi\}, \{\varphi, 0, 2\pi\},\right.$
$\left.\left.\text{Method} \to \text{MultiDimensional}, \text{AccuracyGoal} \to 6, \text{PrecisionGoal} \to 6\right]\right)^{\frac{1}{2}};$
$\text{Print}\left[\text{"}e_{\mathcal{N}}\text{="}, \text{CForm}[\text{Chop}[e, \text{EPS}]], \text{"\%"}\right];$
$e_{\mathcal{N}} = 0.4323351762477782\%$